Cell Reports

Article

The Long Pentraxin 3 (PTX3) Suppresses Immunity to Cutaneous Leishmaniasis by Regulating CD4+ T Helper Cell Response

Graphical Abstract

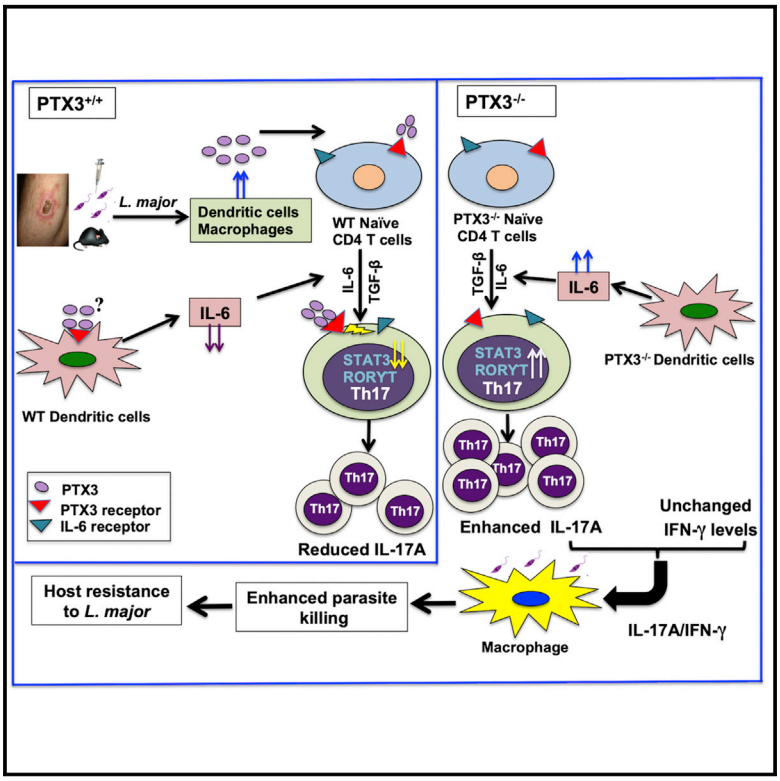

Highlights

- *Leishmania* induces the expression of PTX3 in human and mice cutaneous lesions
- PTX3-deficient mice display enhanced resistance to *Leishmania* infection
- Enhanced resistance is associated with increased IL-17A and Th17 response
- IL-17A synergizes with IFN-γ, leading to macrophage activation and parasite killing

Authors

Gaurav Gupta, Zhirong Mou, Ping Jia, ..., Abdel Soussi-Gounni, Camila I. de Oliveira, Jude E. Uzonna

Correspondence

jude.uzonna@umanitoba.ca

In Brief

Leishmaniasis affects millions of people worldwide. Gupta et al. demonstrate that PTX3, an innate immune molecule, is induced following *Leishmania* infection, resulting in decreased Th17 response and disease susceptibility. Targeted deletion of the *PTX3* gene increases Th17 response and enhances resistance to cutaneous leishmaniasis, demonstrating that PTX3 negatively regulates Th17 response.

Gupta et al., 2020, Cell Reports *33*, 108513
December 15, 2020
https://doi.org/10.1016/j.celrep.2020.108513

CellPress

Cell Reports

CellPress
OPEN ACCESS

Article

The Long Pentraxin 3 (PTX3) Suppresses Immunity to Cutaneous Leishmaniasis by Regulating CD4$^+$ T Helper Cell Response

Gaurav Gupta,[1,2] Zhirong Mou,[1] Ping Jia,[1] Rohit Sharma,[3] Romaniya Zayats,[1] Sayonara M. Viana,[3] Lianyu Shan,[1] Aldina Barral,[3] Viviane S. Boaventura,[3] Thomas T. Murooka,[1] Abdel Soussi-Gounni,[1] Camila I. de Oliveira,[3] and Jude E. Uzonna[1,4,*]

[1]Department of Immunology, Max Rady College of Medicine, Rady Faculty of Health Sciences, University of Manitoba, Winnipeg, MB, Canada
[2]NIIT University, Rajasthan, India
[3]Instituto Gonçalo Muniz (IGM), FIOCRUZ, Salvador, Brazil
[4]Lead Contact
*Correspondence: jude.uzonna@umanitoba.ca
https://doi.org/10.1016/j.celrep.2020.108513

SUMMARY

The long pentraxin 3 (PTX3) plays a critical role in inflammation, tissue repair, and wound healing. Here, we show that PTX3 regulates disease pathogenesis in cutaneous leishmaniasis (CL). PTX3 expression increases in skin lesions in patients and mice during CL, with higher expression correlating with severe disease. PTX3-deficient (*PTX3*$^{-/-}$) mice are highly resistant to *L. major* and *L. braziliensis* infections. This enhanced resistance is associated with increases in Th17 and IL-17A responses. The neutralization of IL-17A abolishes this enhanced resistance, while rPTX3 treatment results in decrease in Th17 and IL-17A responses and increases susceptibility. *PTX3*$^{-/-}$ CD4$^+$ T cells display increased differentiation to Th17 and expression of Th17-specific transcription factors. The addition of rPTX3 suppresses the expression of Th17 transcription factors, Th17 differentiation, and IL-17A production by CD4$^+$ T cells from *PTX3*$^{-/-}$ mice. Collectively, our results show that PTX3 contributes to the pathogenesis of CL by negatively regulating Th17 and IL-17A responses.

INTRODUCTION

Cutaneous leishmaniasis (CL) is caused by several species of protozoan parasites that belong to the genus *Leishmania.* The disease is endemic to the Middle East, Asia, Latin and Central America, and north Africa (Alvar et al., 2012). Resistance to CL is usually associated with the development of strong IFN-γ-producing CD4$^+$Th1 cells, which activate macrophages to produce nitric oxide (NO), an effector molecule for killing intracellular parasites (Locksley et al., 1991, 1993; Reiner and Locksley, 1995; Scott, 1996). In contrast, susceptibility has been associated with interleukin-4 (IL-4) and IL-10 production by T helper 2 (Th2) cells, which are cytokines that deactivate macrophages and inhibit their ability to kill intracellular parasites (Launois et al., 1997; Reiner and Locksley, 1995). Besides Th1 and Th2 cells, IL-17A-secreting Th17 cells have also been shown to mediate either host protection (Banerjee et al., 2018; Nascimento et al., 2015; Pitta et al., 2009; Sheel et al., 2015) or susceptibility (Lopez Kostka et al., 2009; Pedraza-Zamora et al., 2017; Terrazas et al., 2016) to leishmaniasis. However, the series of events that leads to the induction of Th17 responses in CL is unknown. Our group recently showed that Th17 activation and IL-17A production during allergic asthma was regulated in part by the long pentraxin 3 (PTX3) (Balhara et al., 2017), a soluble pattern recognition molecule that forms an integral part of the host innate immunity (Garlanda et al., 2002; Ma et al., 2009). Whether PTX3 also plays a central role in regulating Th17 responses during CL is unknown.

PTX3 is expressed by both immune and non-immune cells, such as myeloid dendritic cells (Doni et al., 2003; Introna et al., 1996), neutrophils (Jaillon et al., 2007), macrophages (Deban et al., 2011), mononuclear phagocytes, endothelial cells (Breviario et al., 1992), smooth muscle cells (Zhang et al., 2015), epithelial cells (dos Santos et al., 2004; Han et al., 2005), fibroblasts (Goodman et al., 2000), and adipocytes (Abderrahim-Ferkoune et al., 2003). PTX3 is involved in pathogen recognition (Diniz et al., 2004; Garlanda et al., 2002; Jeannin et al., 2005) and plays an important protective role in bacterial (Moalli et al., 2011; Soares et al., 2006), fungal (Garlanda et al., 2002; Moalli et al., 2010), and viral (Bozza et al., 2006; Reading et al., 2008) infections by modulating the host inflammatory response. Interestingly, PTX3 is capable of promoting (Souza et al., 2009) as well as suppressing (Dias et al., 2001; Salio et al., 2008) tissue damage due to excessive inflammation, and PTX3 also participates in wound healing and tissue repair (Doni et al., 2016). However, the role of PTX3 in the pathogenesis of protozoan infections is currently unknown.

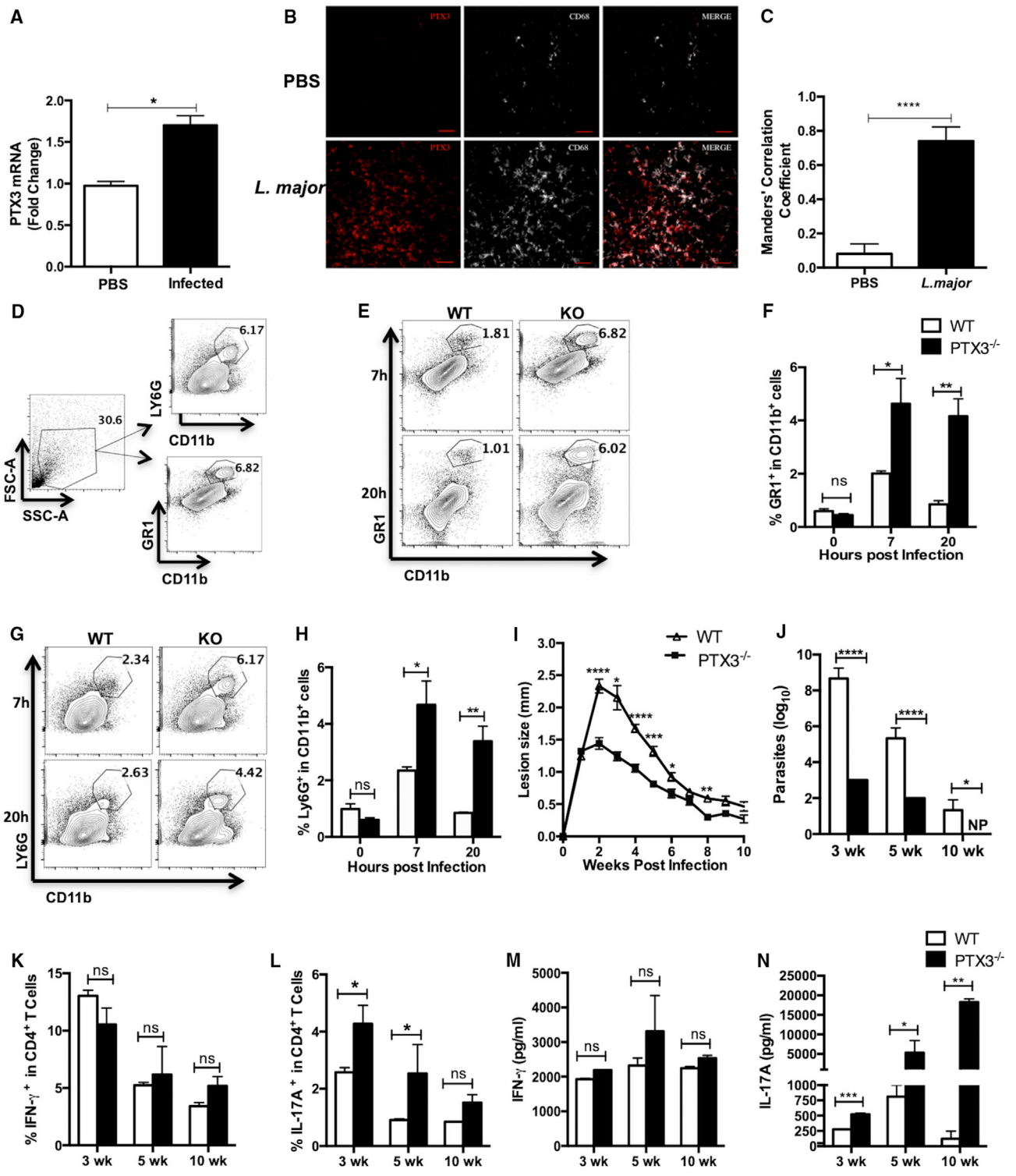

Figure 1. PTX3 Expression Is Increased in CL Lesions and Mediates Susceptibility to *L. major* Infection

(A) Wild-type (WT) C57BL/6 mice (n = 6) were infected in the ear with 2 × 10^6 stationary-phase *L. major* promastigotes, and after 7 days, the expression of PTX3 mRNA at the infection site was assessed by RT-PCR using PBS-treated contralateral ears as controls.

(B) Representative confocal micrographs of ear sections after PBS or *L. major* injection. Ten-micron (10-μm) sections of infected or control ears were stained for PTX3 (red) and CD68 (white) and visualized by confocal microscopy. Scale bar, 20 μm.

(legend continued on next page)

Given the well-characterized roles of PTX3 in inflammation and tissue repair, which are critical physiological events associated with the resolution of skin lesions during CL, we investigated whether PTX3 played a protective or pathogenic role during natural and experimental CL. We show that PTX3 negatively regulates immunity to CL by suppressing Th17 differentiation and IL-17A production by $CD4^+$ T cells, thereby negatively affecting IL-17A augmentation of IFN-γ-mediated macrophage activation, NO production, and parasite destruction.

RESULTS

PTX3 Negatively Regulates the Pathogenesis of Cutaneous Leishmaniasis

PTX3 has been shown to regulate immunity against a wide range of pathogens (Garlanda et al., 2002; Moalli et al., 2010; Soares et al., 2006) and to participate in wound healing and tissue repair (Doni et al., 2016) by modulating the host inflammatory responses. However, its role in the pathogenesis of protozoan infections is unknown. To determine whether PTX3 contributes to disease pathogenesis in CL (a disease characterized by cutaneous inflammation), we determined changes in the levels of PTX3 gene expression during active infections in mice. RT-PCR analysis showed that the level of PTX3 mRNA was significantly increased at the cutaneous site following infection (Figure 1A). Likewise, the expression of PTX3 protein (Figures 1B and 1C) was higher at the site of *L. major* infection compared to uninfected sites, and the expression was mostly restricted to $CD68^+$ (monocytic) cells (Figure 1B). We confirmed PTX3 mRNA expression in macrophages and dendritic cells (DCs) following *L. major* infection *in vitro* (Figure S1).

The increased expression of PTX3 at infected cutaneous sites suggests that it could mediate either host susceptibility or resistance to infection. To determine this, we compared the outcome of *L. major* infection in wild-type (WT) and PTX3-deficient ($PTX3^{-/-}$) mice. At different times after infection, $PTX3^{-/-}$ mice had significantly ($p < 0.01$–0.0001) smaller lesion sizes compared to their WT counterparts (Figure 1I). The smaller lesion size corresponded with significantly ($p < 0.01$–0.0001) lower parasite burden in $PTX3^{-/-}$ mice at 3, 5, and 10 weeks post-infection compared to their WT counterpart mice (Figure 1J). Interestingly, there was no gene dose effect, as infected heterozygote ($PTX3^{+/-}$) mice showed a phenotype similar to infected WT mice (Figures S2A and S2B). $PTX3^{-/-}$mice also displayed enhanced resistance to low-dose intradermal *L. major* infection (Figure S3). Furthermore, during the early time points of *L. major* infection, $PTX3^{-/-}$ mice had a higher frequency of inflammatory neutrophils $GR1^+$ and $Ly6G^+CD11b$ cells (Figures 1F, 1H, S4A, and S4B) at the infection site compared to their WT control mice. These results indicate that PTX3 negatively regulates disease pathogenesis and possibly immunity during CL.

Enhanced Resistance in PTX3-Deficient Mice Is Associated with Increased IL-17A Production

Since resistance to CL is usually associated with robust interferon-γ (IFN-γ) and tumor necrosis factor-α (TNF-α) and reduced IL-10 production by $CD4^+$ T cells, we assessed the frequency of cells producing these cytokines in infected WT and $PTX3^{-/-}$ mice. Surprisingly, we observed comparable frequencies of IFN-γ^+CD4^+ and TNF-α^+CD4^+ T cells (Figures 1K and S2–S5) in both the spleens and draining lymph nodes (dLNs) from infected WT and $PTX3^{-/-}$ mice when assessed directly *ex vivo*. Interestingly, we found that infected $PTX3^{-/-}$ mice had significantly ($p < 0.05$) higher frequencies of IL-$17A^+CD4^+$ T cells at 3, 5, and 10 weeks post-infection compared to their WT counterparts (Figure 1L). This was consistent with significantly elevated levels of IL-17A (Figure 1N) in the culture supernatant fluids of soluble *Leishmania* antigen (SLA)-stimulated splenocytes isolated from infected $PTX3^{-/-}$ mice. In contrast and consistent with the flow cytometry data, the levels of IFN-γ (Figure 1M) in the culture supernatant fluids were comparable between WT and $PTX3^{-/-}$ mice. We observed a lower frequency of IL-10^+CD4^+ T cells in the spleens and dLNs of infected $PTX3^{-/-}$ mice at 3 weeks post-infection compared to WT mice. In line with this, IL-10 levels in the culture supernatant fluids of cells from infected $PTX3^{-/-}$ mice were lower than those from WT mice at 3 weeks post-infection (Figure S6). However, these differences were not observed at later time points during the chronic phase of the disease (Figure S6).

Collectively, these results indicated that the enhanced resistance to *L. major* infection in $PTX3^{-/-}$ mice was not due to enhanced Th1 response, but rather is associated with stronger Th17 response and a transient suppression of IL-10 response in the absence of PTX3 signaling.

PTX3 Deficiency Enhances Th17, but Does Not Affect Th1 Polarization *In Vitro*

Given that we found enhanced IL-17 production following *L. major* infection of $PTX3^{-/-}$ mice, we speculated that PTX3

(C) Manders' overlap coefficient (MOC) quantifying the degree of co-localization of PTX3 signals in $CD68^+$ cells. Some infected mice were sacrificed at 7 and 20 h post-infection, and the frequency of $CD11b^+$ cells in the infected ears were analyzed by flow cytometry.

(D–H) Gating strategy (D), contour plots (E and G), and bar graphs (F and H) representing the percentages of $GR1^+$ (E and F) and $Ly6G^+$ cells (G and H) in the infected ears.

(I) WT and $PTX3^{-/-}$ mice were infected in the footpad with 2×10^6 stationary-phase *L. major* promastigotes and lesion size was measured weekly with digital calipers.

(J) At the indicated times, some infected mice (n = 5 mice per each time point) were sacrificed, and parasite burden in the infected sites was quantified by limiting dilution.

(K and L) At sacrifice, the frequency of IFN-γ^+ (K) and IL-$17A^+$ (L)-producing $CD4^+$ T cells in the spleens of infected WT and $PTX3^{-/-}$ mice were analyzed directly *ex vivo* by flow cytometry.

(M and N) The spleen cells were also restimulated *in vitro* with SLA (50 μg/mL) for 72 h, and the levels of IFN-γ (M) and IL-17A (N) in the cell culture supernatant fluids were determined by ELISA.

Results are representative of 2 (A–H) and 3 (I–N) independent experiments with similar results. *$p < 0.05$; **$p < 0.01$; ***$p < 0.005$; and ****$p < 0.0001$. NS, not significant. Data are expressed as means ± standard errors. NP, no parasites detected.

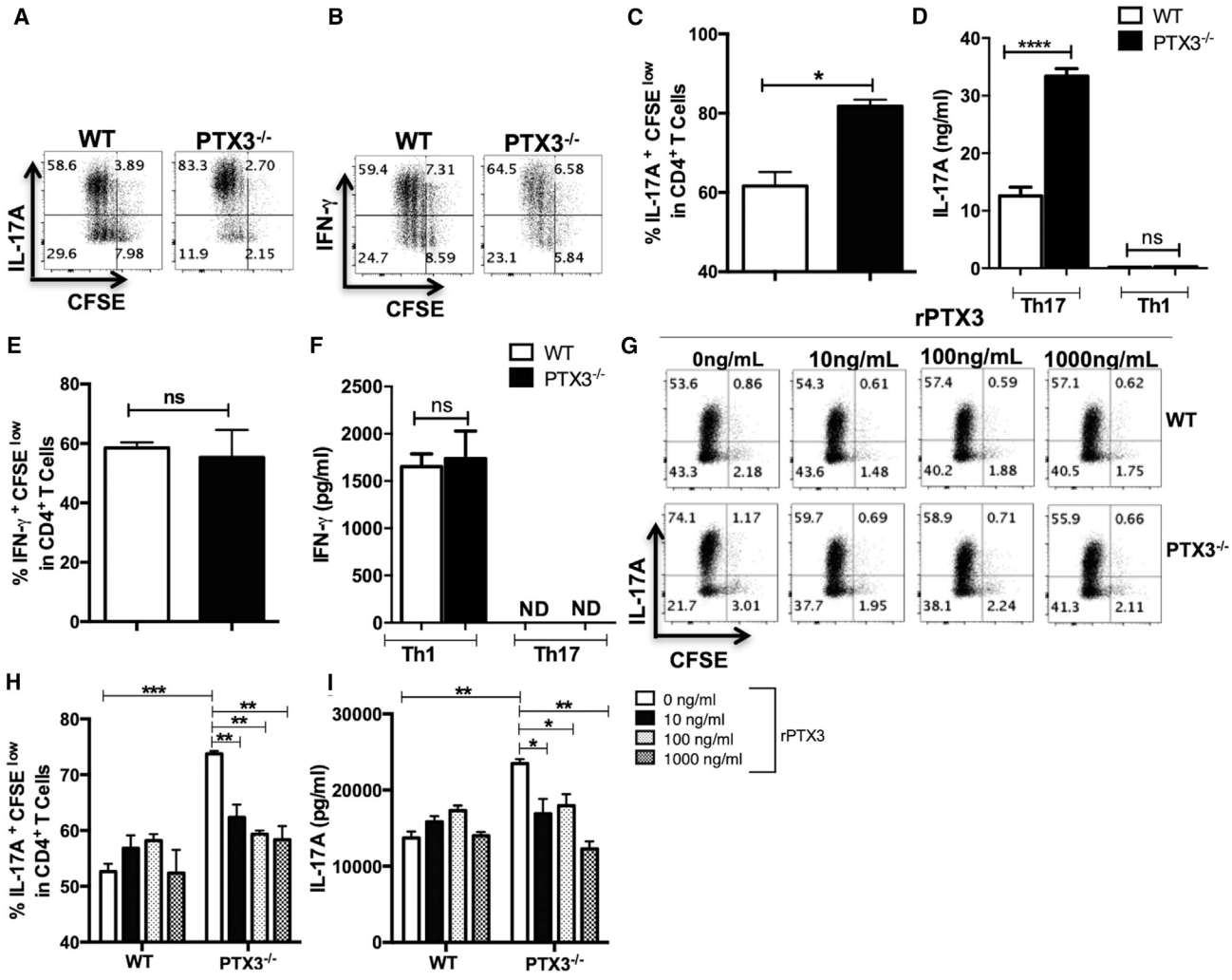

Figure 2. Deficiency of PTX3 Enhances Th17 Differentiation *In Vitro*

Splenocytes from WT and *PTX3*$^{-/-}$ mice were labeled with carboxyfluorescein succinimidyl ester (CFSE) dye and stimulated *in vitro* with soluble anti-CD3 and anti-CD28 antibodies under Th1 or Th17 polarizing conditions. After 72 h, the frequencies of IFN-γ- and IL-17A-secreting CD4$^+$ T cells were determined by flow cytometry. Representative dot plots (A and B) and bar graphs (C and E) show the percentage of CFSE^{lo}IL-17A$^+$ (A and C) and CFSE^{lo}IFN-γ$^+$ (B and E) CD4$^+$ T cells. The levels of IL-17A (D) and IFN-γ (F) in the culture supernatant fluids were assayed by ELISA. In some experiments, Th17 polarization was performed in the presence or absence of different concentrations of rPTX3 (G and H), and after 72 h, the frequency of IL-17A-secreting CD4$^+$ cells was determined by flow cytometry. Representative dot plots (G) and bar graphs (H) show the percentage of CFSE^{lo}CD4$^+$IL-17A$^+$ T cells. The levels of IL-17A in the culture supernatant fluids were measured by ELISA (I). The results are representative of 3 independent experiments with similar results. *$p < 0.05$; **$p < 0.01$; and ****$p < 0.0001$. NS, not significant. Data are expressed as means ± standard errors.

may negatively regulate Th17 response. To test this, we performed *in vitro* Th17 and Th1 polarization studies using splenocytes obtained from WT and *PTX3*$^{-/-}$ mice. Data presented in Figures 2A and 2C show significantly ($p < 0.03$) higher frequencies of CFSE^{lo}CD4$^+$IL-17A$^+$ (Th17) cells in splenocytes from *PTX3*$^{-/-}$ mice compared to their WT counterpart mice. In contrast and consistent with mouse infection results, the frequency of CFSE^{lo}CD4$^+$IFN-γ$^+$ (Th1) cells in both WT and *PTX3*$^{-/-}$ splenocytes under Th1 polarizing conditions were comparable (Figures 2B and 2E). We confirmed these findings by ELISA, which showed higher levels of IL-17A in cell culture supernatant fluids of splenocytes from *PTX3*$^{-/-}$ mice under Th17 polarizing conditions (Figure 2D) but comparable levels of IFN-γ in both WT and *PTX3*$^{-/-}$ splenocytes under Th1 polarizing conditions (Figure 2F). We also observed similar increased frequency of Th17 cells using purified CD4$^+$T cells from *PTX3*$^{-/-}$ spleens under Th17 polarizing conditions, and this was blocked in a dose-dependent manner by rIL-17 (Figure S7). These results show that deficiency of PTX3 potentiates Th17 differentiation and IL-17A production.

The preceding findings suggest that PTX3 may be a negative regulator of Th17 response. To directly test this, we added recombinant PTX3 (rPTX3) to cultures of WT and *PTX3*$^{-/-}$ splenocytes under Th17 polarization conditions. The addition of rPTX3

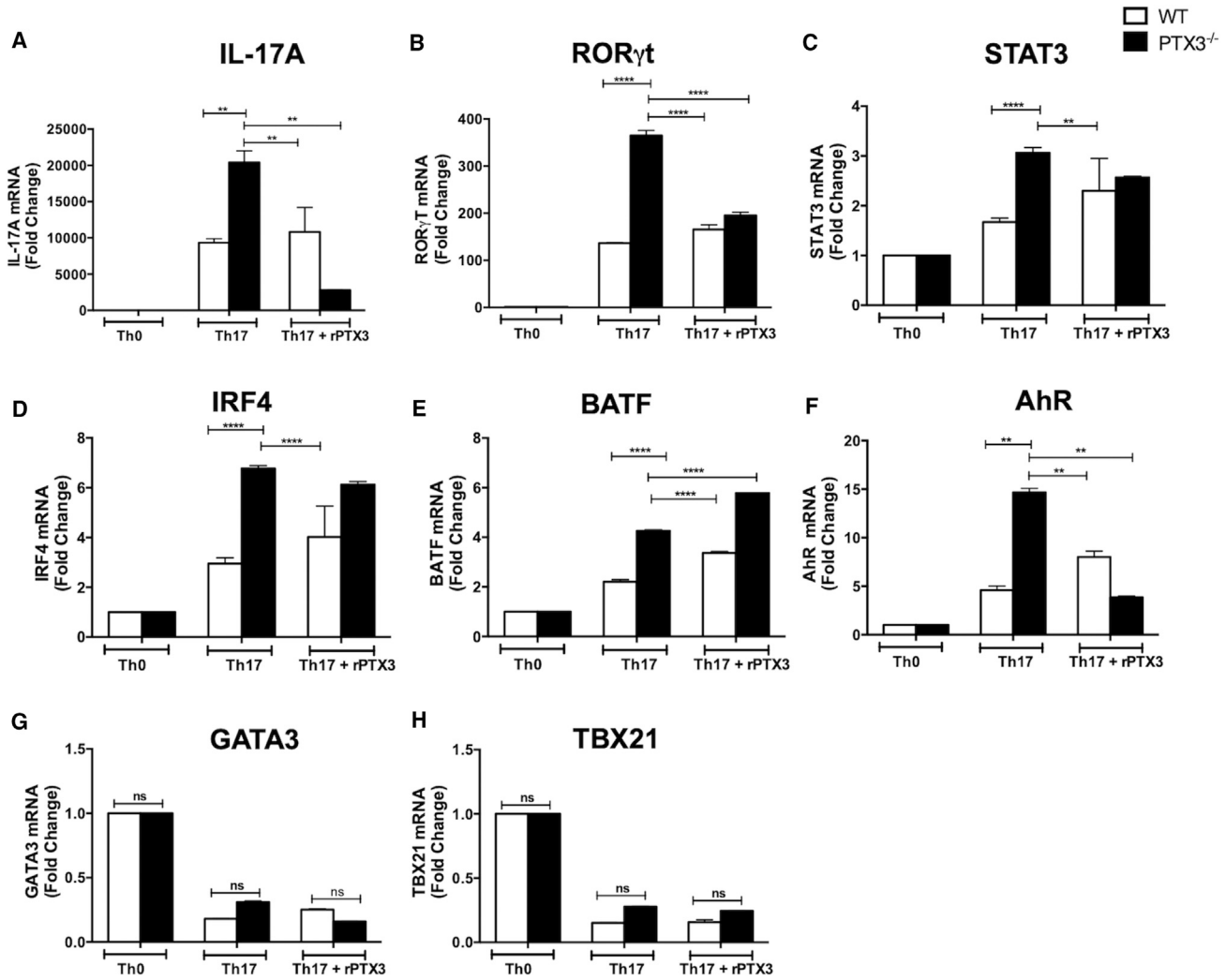

Figure 3. PTX3 Negatively Regulates Th17-Specific Transcription

Splenocytes from WT and *PTX3*$^{-/-}$ mice were stimulated with soluble anti-CD3 and anti-CD28 antibodies under Th17 polarizing conditions in the presence or absence of rPTX3 (200 ng/mL). After 72 h, total RNA was isolated from the cells and mRNA levels of IL-17A (A), RORγt (B), STAT3 (C), IRF4 (D), BATF (E) AhR (F), GATA3 (G), and TBX21 (H) were determined by RT-PCR. Results are representative of 3 independent experiments with similar results. **$p < 0.01$; ***$p < 0.005$; and ****$p < 0.0001$. NS, not significant. Data are expressed as means ± standard errors.

significantly reduced the frequency of Th17 cells and the production of IL-17A by whole splenocytes (Figures 2G–2I) or purified CD4$^+$ T cells (Figure S7) from *PTX3*$^{-/-}$ mice. Collectively, these findings directly confirm that PTX3 is a negative regulator of Th17 differentiation and IL-17 production by CD4$^+$ T cells.

PTX3 Negatively Regulates Th17-Specific Transcription Factors

The observation that rPTX3 suppressed the polarization of purified CD4$^+$ T cells from *PTX3*$^{-/-}$ mice into Th17 cells suggests that it may directly affect crucial transcription factors involved in the differentiation of CD4$^+$ T cells into Th17 cells. Therefore, we performed RT-PCR to determine mRNA levels of key Th17 transcription factors in WT and *PTX3*$^{-/-}$ splenocytes under Th17 polarizing conditions in the presence or absence of rPTX3. As expected, there was significantly increased mRNA expression of IL-17A in total splenocytes (Figure 3A) or purified CD4$^+$ T cells (Figure S8) from *PTX3*$^{-/-}$ mice compared to those from their WT counterpart mice following *in vitro* Th17 differentiation, and this was inhibited by the addition of rPTX3. Concomitantly, there was ~2- to 4-fold higher expression of RORγt, STAT3, IRF4, BATF, and AhR mRNA in Th17 polarized whole splenocytes (Figures 3B–3F) or purified CD4$^+$ T cells (Figure S8) from *PTX3*$^{-/-}$ mice compared to those from WT mice. The addition of rPTX3 to *PTX3*$^{-/-}$ splenocytes resulted in the significant inhibition of IL-17A mRNA and a concomitant decrease in RORγt and AhR mRNA levels in comparison to untreated controls (Figures 3A, 3B, and 3F). Reductions in the levels of STAT3 and IRF4 mRNA were also observed in rPTX3-treated cells from *PTX3*$^{-/-}$ mice, although these were

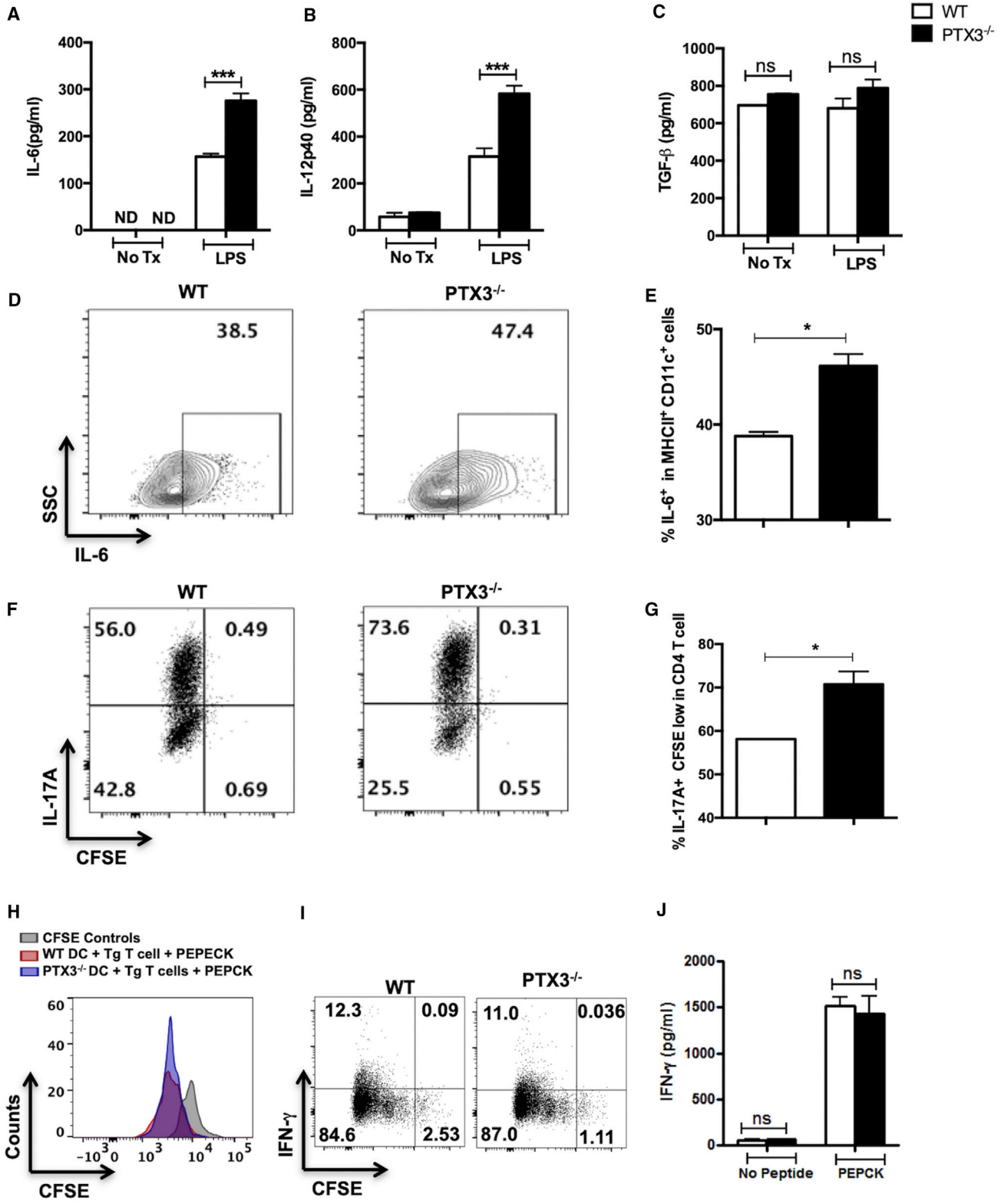

Figure 4. PTX3 Regulates IL-12 and IL-6 Production by Dendritic Cells (DCs)

(A–C) Highly purified splenic CD11c$^+$ cells from naive WT and *PTX3*$^{-/-}$ mice were either unstimulated (NoTx) or stimulated with LPS (1 μg/mL), and after 24 h, the cell culture supernatant fluids were collected and assayed for IL-6 (A), IL-12p40 (B), and transforming growth factor-β (TGF-β) (C) by sandwich ELISA. WT and

(legend continued on next page)

not statistically significant (Figures 3C and 3D), while rPTX3 increased the expression of BATF mRNA (Figure 3E). In contrast, mRNA levels of GATA3 and TBX21, key transcription factors for the differentiation of Th2 and Th1 cells, respectively, were not different between WT and *PTX3*$^{-/-}$ mice (Figures 3G, 3H, and S8). These findings show that PTX3 negatively regulates Th17 responses by downregulating the expression of some key IL-17A-specific transcription factors.

Dendritic Cells from *PTX3*$^{-/-}$ Mice Produce More IL-6 and Contribute to Increased Th17 Responses

DCs present pathogen-derived antigenic peptides to naive CD4^{+} T cells to initiate antigen-specific Th cell activation and differentiation toward specific effector subsets (Merad et al., 2013; Okwor et al., 2015; Sia et al., 2015; Srivastava et al., 2014; Xu et al., 2007). Because we found that the absence of PTX3 augmented Th17 responses, we assessed whether the deficiency of PTX3 affected DC responses in a way that favors Th17 differentiation. Infected *PTX3*$^{-/-}$ mice had significantly more CD11c^{+} cells at the infection site compared to their infected WT counterpart mice (Figure S4B). Splenic CD11c^{+} cells from *PTX3*$^{-/-}$ mice produced higher amounts of IL-6 (Figure 4A) and IL-12p40 (Figure 4B) compared to those from WT mice following lipopolysaccharide (LPS) stimulation. Similarly, the expression of IL-6 by MHC-II^{+}CD11c^{+} cells (Figures 4D and 4E) at the cutaneous site of *L. major* infection was significantly ($p < 0.05$) higher in infected *PTX3*$^{-/-}$ mice compared to their WT counterpart controls. These observations suggest that the deficiency of PTX3 leads to enhanced levels of IL-6 in DCs during *L. major* infection, which could further contribute to increased Th17 responses in these mice. To confirm this, we co-cultured DCs from WT and *PTX3*$^{-/-}$ mice with phosphoenolpyruvate carboxykinase (PEPCK)-specific T cell receptor (TCR)-transgenic CD4^{+} T cells in the presence of the PEPCK peptide. We observed higher frequencies of CD4^{+}IL-17A^{+} T cells in co-cultures of *PTX3*$^{-/-}$ DCs and PEPCK TCR-transgenic CD4^{+} T cells compared to those of WT DCs (Figures 4F and 4G). However, we also observed comparable frequencies of CD4^{+}IFN-γ^{+} T cells in both the co-cultures of *PTX3*$^{-/-}$ DCs with PEPCK TCR-transgenic CD4^{+} T cells and WT DCs with PEPCK TCR-transgenic CD4^{+} T cells (Figures 4H and 4I). Collectively, these findings confirm that *PTX3*$^{-/-}$ DCs are capable of augmenting Th17 responses during *L. major* infection, possibly via regulating IL-6 production.

Enhanced IL-17A Response Contributes to Increased Resistance of *PTX3*$^{-/-}$ Mice to *L. major* Infection

Although some reports suggest that IL-17 plays a pathogenic role in leishmaniasis (Lopez Kostka et al., 2009; Pedraza-Zamora et al., 2017; Terrazas et al., 2016), others show that they play a protective role (Banerjee et al., 2018; Nascimento et al., 2015; Pitta et al., 2009). Because we found that the enhanced resistance of *PTX3*$^{-/-}$ mice to *L. major* was not associated with superior IFN-γ and/or TNF-α response (Figures 1K, 1M, and S2–S5), we postulated that the enhanced resistance was mediated by increased IL-17 response. To test this, we performed *in vivo* neutralization of IL-17A in *L. major*-infected WT and *PTX3*$^{-/-}$ mice. IL-17A neutralization in infected *PTX3*$^{-/-}$ mice resulted in susceptibility as evidenced by higher lesion size (Figure 5A) and parasite burden (Figure 5B) as compared to untreated *PTX3*$^{-/-}$ mice.

Next, we evaluated whether administration of rPTX3 to WT mice could lead to increased susceptibility to *L. major* infection. We infected WT mice with *L. major* and administered rPTX3 intralesionally once per week for 3 weeks. WT mice treated with rPTX3 had increased lesion size (Figure 5C) that corresponded with significantly increased parasite burden (Figure 5D) compared to PBS-treated controls. The enhanced susceptibility following rPTX3 treatment was accompanied by significant ($p < 0.05$) reduction in the frequency of CD4^{+}IL-17A^{+} T cells in the dLNs and spleen compared to PBS-treated controls (Figures 5E and S9). Consistent with previous findings (Figures 2B and 2F), there was no difference in the frequency of CD4^{+}IFN-γ^{+} T cells in dLNs and spleens of both rPTX3- and PBS-treated groups (Figures 5F and S9). We confirmed the above results by ELISA, which showed increased levels of IL-17A (Figures 5G and S9) and unchanged levels of IFN-γ (Figures 5H and S9) in cell culture supernatant fluids of SLA-stimulated dLN and spleen cells from rPTX3-treated mice. These findings confirm that PTX3 enhances susceptibility to *L. major* infection by downregulating the IL-17A response.

IL-17A Synergizes with IFN-γ to Mediate Effective Parasite Killing in Macrophages

Leishmania resides inside host macrophages, and their clearance requires the activation of infected cells by IFN-γ, leading to the production of reactive oxygen and nitrogen intermediates (Gupta et al., 2013). To fully understand how the deficiency of PTX3 enhances resistance to *L. major* infection, we compared the uptake, replication, and killing of parasites in macrophages from WT and *PTX3*$^{-/-}$ mice. Both WT and *PTX3*$^{-/-}$ macrophages had similar parasite uptake as seen by equivalent numbers of amastigotes in WT and *PTX3*$^{-/-}$ cells at all time points (6, 24, 48, and 72 h post-infection, Figures 6A and 6B), suggesting that the deficiency of PTX3 had no effect on infectivity and parasite proliferation inside infected cells. Furthermore, both infected WT and *PTX3*$^{-/-}$ macrophages had a comparable ability to kill parasites following activation with LPS or IFN-γ (Figure 6C).

Because IL-17 has been proposed to enhance leishmanicidal activity (Nascimento et al., 2015), we examined whether the

PTX3$^{-/-}$ mice were infected in the ear with 2 × 10^{6} stationary phase *L. major* promastigotes, and after 4 weeks, spleen cells were assessed for the frequency of IL-6 producing MHCII^{+}CD11c^{+}cells by flow cytometry.

(D and E) Representative contour plots (D) and bar graph (E) showing the percentage of MHCII^{+}CD11c^{+}IL-6^{+} cells. Bone marrow-derived DCs (BMDCs) from WT and *PTX3*$^{-/-}$ mice were co-cultured with CFSE-labeled PEPCK-specific T cell receptor transgene (TCRTg) CD4^{+} T cells at a 1:10 ratio in the presence of PEPCK peptide (5 μM) under Th17 polarizing conditions. After 72 h, the frequency of CD4^{+}IL-17A^{+}and CD4^{+}IFN-γ^{+} T cells was determined by flow cytometry.

(F–I) Shown are representative dot plots (F and I) and bar graph (G) representing the percentage of CFSE^{lo}CD4^{+}IL-17A^{+} (F and G) and CFSE^{lo}CD4^{+}IFN-γ^{+} (H and I) T cells.

(J) The levels of IFN-γ in the culture supernatant fluids from the above co-culture sets were measured by ELISA.

Results are representative of 2 independent experiments with similar results. *$p < 0.05$ and ***$p < 0.005$. NS, not significant. Data are expressed as means ± standard errors.

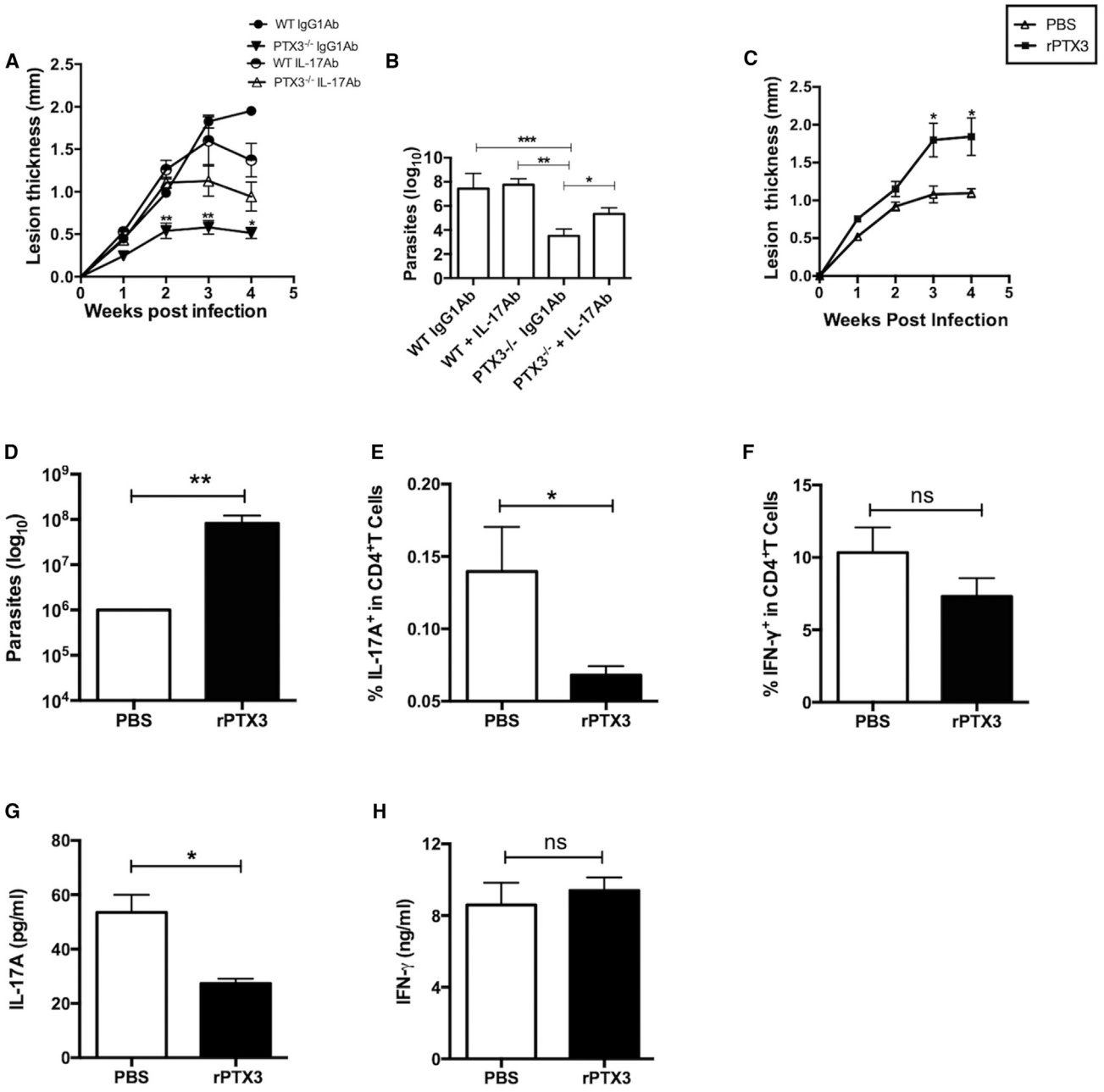

Figure 5. *In Vivo* Neutralization of IL-17A or rPTX3 Treatment Increase Susceptibility to *L. major* Infection

WT and *PTX3*$^{-/-}$ mice (n = 5 per group) were treated (intraperitoneally [i.p.]) with either control immunoglobulin (Ig) or anti-IL-17A neutralizing monoclonal antibody (mAb) 1 day before infection in the footpad with 2 × 10^6 *L. major* stationary phase promastigotes. Anti-IL17 mAb treatment was continued once weekly for an additional 4 weeks.

(A and B) The lesion size (A) was measured weekly and mice were sacrificed after 4 weeks to estimate parasite burden (B). Groups of WT mice were infected in the footpad with *L. major* and 1 day post-infection, mice were divided into 2 groups (6 mice/group) and treated intralesionally with either PBS or rPTX3 (0.5 μg/mouse) 3 times weekly.

(C and D) Lesion size (C) was measured weekly, and after 4 weeks, mice were sacrificed and parasite burden was determined by limiting dilution (D).

(E and F) At sacrifice, cells from the dLNs were assessed directly *ex vivo* for the frequency of IL-17$^+$ (E) and IFN-γ$^+$ (F) producing CD4$^+$ T cells by flow cytometry.

(G and H) Some dLN cells were restimulated *in vitro* with SLA (50 μg/mL) for 72 h, and the levels of IL-17A (G) and IFN-γ (H) in the cell culture supernatant fluids were determined by ELISA.

Results are representative of 2 independent experiments with similar results. *p < 0.05; **p < 0.01; and ***p < 0.005. NS, not significant. Data are expressed as means ± standard errors.

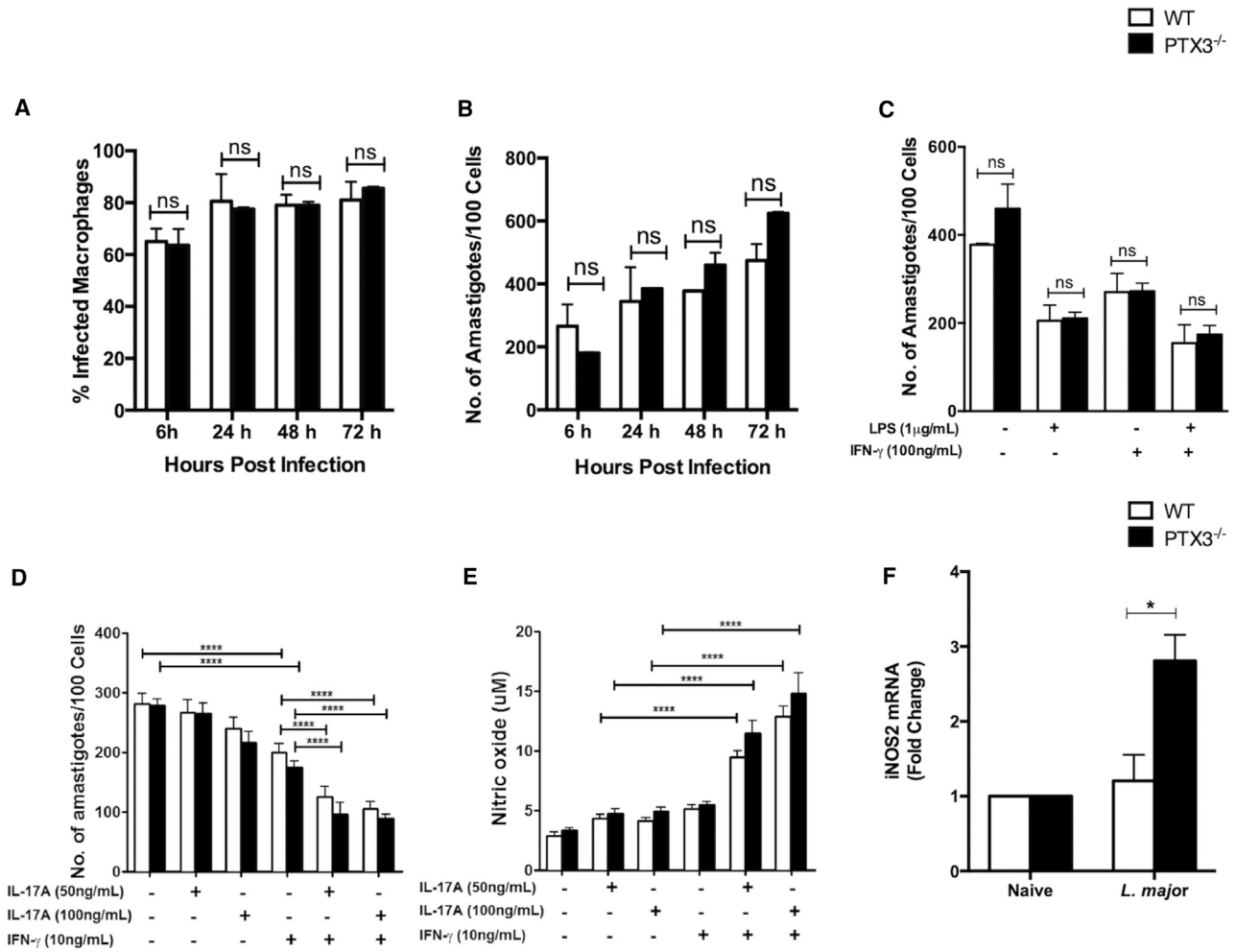

Figure 6. PTX3 Synergizes with IFN-γ to Mediate Killing of *L. major* in Infected Macrophages

(A and B) BMDMs from WT and *PTX3*$^{-/-}$ mice were infected with *L. major*, and at indicated times, cytospin preparations were stained with Wright-Giemsa stain and the percent infection (A) and total number of parasites per 100 cells (B) were determined by microscopy.

(C) In another independent experiment, infected bone marrow-derived macrophages from WT and *PTX3*$^{-/-}$ mice were stimulated with either LPS (1 μg/mL), IFN-γ (100 ng/mL) or both for 48 h and the number of parasites per 100 cells was determined.

(D and E) BMDMs from WT and *PTX3*$^{-/-}$ mice were infected with *L. major* in the presence or absence of IL-17A (50 and 100 ng/mL) or IFN-γ (10 ng/mL) alone or both. After 48 h, cytospin preparations were stained with Wright-Giemsa stain, and the number of parasites per 100 cells was determined by microscopy (D) and the concentration of nitrite in the supernatant fluid was determined (E).

(F) WT mice (n = 4) were infected in the footpad with 2 × 10^6 stationary phase *L. major* promastigotes, and after 4 weeks, the expression of iNOS2 mRNA at the infection site was assessed by RT-PCR using PBS-treated contralateral footpads as controls.

Data are shown as means ± SEMs of 4–6 infection tubes/group and are from a single experiment representative of at least 3 independent experiments. *p < 0.05 and ****p < 0.0001. NS, not significant.

enhanced resistance to *L. major* in *PTX3*$^{-/-}$ mice was related to the IL-17 augmentation of IFN-γ-mediated *Leishmania* killing activity. We primed WT and *PTX3*$^{-/-}$ bone marrow-derived macrophages (BMDMs) with IL-17 (50 and 100 ng/mL) in the presence or absence of a suboptimal dose of IFN-γ (10 ng/mL) and infected them with *L. major*. The results presented in Figures 6D and 6E show that IL-17 synergizes with suboptimal doses of IFN-γ to mediate more effective parasite killing and increased NO production (compared to treatment with IFN-γ or IL-17 alone). Similarly, we observed increased inducible NO synthase 2 (iNOS2) mRNA expression at the site of infection in *PTX3*$^{-/-}$ mice compared to WT counterparts (Figure 6F), which confirmed our *in vitro* findings. Our results show that the enhanced resistance of *PTX3*$^{-/-}$ mice to *L. major* is due to enhanced IL-17A production, which synergizes with IFN-γ to enhance NO production, leading to more effective killing of parasites in infected macrophages.

PTX3 Expression Is Increased in Skin Lesions and Correlates with Disease Severity in Patients with Cutaneous Leishmaniasis

Increased IL-17A levels have been shown to correlate with better disease outcomes in patients with subclinical *L. braziliensis*

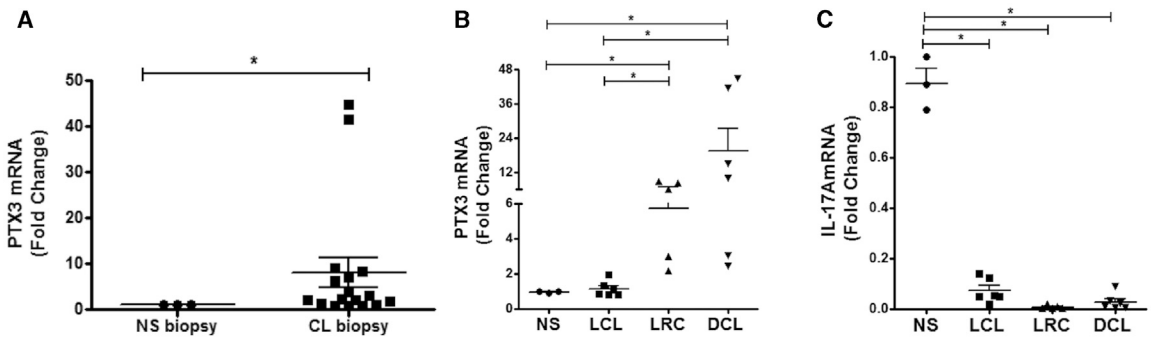

Figure 7. PTX3 mRNA Level Is Increased in CL Lesions of Patients and Directly Correlates to Disease Severity

(A) Skin biopsies from normal patients (n = 3) and patients with CL caused by *L. braziliensis* (n = 17) were assessed for expression levels of PTX3 mRNA by RT-PCR (A).

(B and C) PTX3 (B) and IL-17A (C) mRNA levels in biopsies from normal patients (NS) (n = 3) and patients with different forms of CL: localized CL (LCL, n = 6), *Leishmania* recidiva cutis (LRC, n = 5) and disseminated leishmaniasis (DCL, n = 6).

*$p < 0.05$. NS, not significant. Data are expressed as scatterplots showing means ± standard deviations.

infection (Novoa et al., 2011), and IL-17A (possibly derived from Th17 cells) has been shown to mediate protective immunity in patients against *L. infantum, L. major*, and human post-kala-azar dermal leishmaniasis (Gonzalez-Lombana et al., 2013; Nascimento et al., 2015; Pitta et al., 2009). We found that *PTX3*$^{-/-}$ mice infected with *L. braziliensis* harbor a significantly lower parasite burden compared to their infected WT counterpart mice and that this was associated with a significantly higher frequency of IL-17A-producing CD4$^+$ T cells in their spleens and dLNs (Figure S10). Given that we found that PTX3 expression negatively regulates IL-17A expression, we assessed the expression of PTX3 and IL-17A mRNA in skin biopsies from patients with CL and whether this correlates with disease severity. The level of PTX3 mRNA was significantly higher (15-fold, $p < 0.01$) in skin biopsies taken from cutaneous lesions from *L. braziliensis*-infected patients compared to healthy controls (Figure 7A) and correlates with disease severity such that the levels were highest in individuals with disseminated CL (DCL), which is the most severe form of the disease (Figure 7B). PTX3 expression was associated with significant suppression (undetectable levels) of IL-17A mRNA in the skin biopsies from infected patients compared to healthy controls (Figure 7C). These results indicate that PTX3 negatively regulates disease pathogenesis during CL by suppressing IL-17A production.

DISCUSSION

Here, we showed that PTX3 levels were elevated in skin lesions from patients and mice suffering from CL, suggesting that this innate pattern recognition molecule may play a critical role in disease pathogenesis. Using a loss-of-function approach, we showed that the deficiency of PTX3 resulted in enhanced resistance to *L. major*, and this was associated with an increased IL-17 (but not IFN-γ and TNF-α) response. Neutralization studies showed that the enhanced resistance of *PTX3*$^{-/-}$ mice to *L. major* is due to enhanced Th17 responses in these mice. In contrast, the administration of rPTX3 led to an increased susceptibility to *L. major*, which was associated with a dramatic down-regulation of Th17 responses and IL-17A production by lymph node cells draining the infection site. Using an *in vitro* approach, we showed that CD4$^+$ T cells from *PTX3*$^{-/-}$ mice showed enhanced expression of Th17 transcription factors that drive Th17 differentiation. These results show, for the first time, that PTX3 is a negative regulator of Th17 response during CL and contributes to disease severity.

The expression of PTX3, a key molecule of the innate immune defense system, is upregulated in response to different stimuli such as inflammatory cytokines (IL-1β, TNF-α), Toll-like receptor (TLR) agonists (e.g., LPS), distinct microbial associated molecular patterns (e.g., OmpA, lipoarabinomannans), and some pathogens (*Escherichia coli*, *Staphylococcus aureus*) (Bottazzi et al., 2010; Garlanda et al., 2005; Inforzato et al., 2011; Jaillon et al., 2007). Studies with *PTX3*$^{-/-}$- and *PTX3*-overexpressing mice have shown that PTX3 mediates protective immunity to various pathogens, including influenza virus, *Aspergillus fumigates*, and *Pseudomonas aeruginosa* (Garlanda et al., 2002; Reading et al., 2008). While correlative studies in human leishmaniasis patients suggest that PTX3 may play a key role in disease pathogenesis, no study has directly demonstrated this and/or showed the mechanism through which this would occur. Results from our studies clearly show that *Leishmania* infection induces PTX3 expression at the cutaneous site of infection, and this blocks effective parasite control by suppressing protective Th17 and IL-17A responses.

IL-17A is a proinflammatory cytokine produced primarily by CD4$^+$ Th17 cells, although other cell types, such as CD8$^+$ T cells, γδ T cells, invariant natural killer T (iNKT) cells, and neutrophils are known to also secrete it. Binding of IL-17A to the IL-17 receptor, which is expressed on many cells, including macrophages, initiates a strong signaling cascade that leads to the expression of inducible NOS, granulocyte-macrophage colony-stimulating factor (GM-CSF), proinflammatory cytokines, antimicrobial peptides, and chemokines (Kolls and Lindén, 2004; Mengesha and Conti, 2017) that are important for host protection from many pathogens such as bacteria (Priebe et al., 2008), fungi

(Conti et al., 2009), and trypanosomes (Cai et al., 2016). We showed the PTX3 negatively regulates IL-17A production during *L. major* infection since its deficiency led to the increased frequency of IL-17A-producing $CD4^+$ T cells in the dLNs and spleens of infected mice. In support of this, we found that the increased expression of PTX3 mRNA in biopsy samples from DCL patients was associated with the suppression of IL-17A mRNA in these tissues. The neutralization of IL-17A abolished the enhanced resistance of infected *PTX3*$^{-/-}$ mice, while rIL-17A treatment conferred enhanced resistance to WT mice as evidenced by significantly reduced lesion size and parasite burden. Furthermore, we found that IL-17A synergizes with IFN-γ to mediate increased NO production and a concomitant more efficient parasite killing in infected macrophages.

The role of IL-17 in the pathogenesis of CL is controversial. While a report suggests that IL-17A mediates susceptibility to *L. major* infection in mice by regulating CXCL2 levels and neutrophil migration to the site of infection (Lopez Kostka et al., 2009), observations in human patients suggest that IL-17A expression may contribute to better disease outcomes. Increased IL-17A levels has been shown to correlate with better disease outcomes in subclinical *L. braziliensis* patients (Novoa et al., 2011). Similarly, studies have shown that IL-17A (possibly derived from Th17 cells) mediates protective immunity in patients against *L. infantum, L. major*, and human post-kala-azar dermal leishmaniasis (Gonzalez-Lombana et al., 2013; Nascimento et al., 2015; Pitta et al., 2009). In line with this, we found that the expression of IL-17A mRNA was highly suppressed in tissue biopsies from DCL patients, which is the most severe form of CL. Our findings that the deficiency of PTX3 was associated with the significant upregulation of Th17 and IL-17 responses that synergize with IFN-γ to cause a more efficient parasite control in macrophages, leading to enhanced resistance, are at odds with a recent report that found that the global deletion of the *IL-17A/F* gene in C57BL6 mice had no impact on the outcome of *L. major* infection (Dietze-Schwonberg et al., 2019). These differences could be due to the fact that in contrast to *IL-17A/F*$^{-/-}$ mice (which completely lack IL-17 production), *PTX3*$^{-/-}$ mice were capable of producing IL-17A. In fact, the levels of IL-17 were significantly higher in *PTX3*$^{-/-}$ mice compared to *PTX3*$^{+/+}$ mice. It is conceivable that the elevated levels of IL-17 in infected *PTX3*$^{-/-}$ mice could produce different physiologic effects compared to low levels as seen in WT mice.

The pathways leading to IL-17A production in *Leishmania*-infected mice and patients are not known. In the present study, we showed that PTX3 is a key molecule that regulates IL-17A response in CL. The expression of PTX3 in cutaneous lesions was directly correlated with the extent of clinical pathology, such that PTX3 levels were highest in patients displaying disseminated (Carvalho et al., 1994; Turetz et al., 2002) and recidivous lesions (Bittencourt et al., 1993). In contrast, PTX3 levels were inversely correlated with the level of IL-17A, such that individuals exhibiting disseminated disease had undetectable levels of IL-17 mRNA in their lesions. The treatment of mice with rPTX3 resulted in enhanced susceptibility to *L. major* infection due to suppressed Th17 responses. These findings are consistent with previous studies on *Aspergillus*, in which rPTX3 treatment led to the suppression of Th17 responses (D'Angelo et al., 2009).

Th17 cell differentiation is driven by TGF-β and IL-6 (Bettelli et al., 2006; Ivanov et al., 2006) and regulated by some key transcription factors, including RORγt (Ivanov et al., 2006), STAT3 (Yang et al., 2007), IRF4 (Brüstle et al., 2007), BATF (Schraml et al., 2009), and AhR (Quintana et al., 2008). In the presence of IL-6 and TGF-β, the cooperative binding of BATF, IRF4, and STAT3 with AhR contributes to initial chromatin accessibility and subsequent recruitment of RORγt to regulate the activation of Th17-relevant genes (Ciofani et al., 2012; Liu et al., 2017). We observed an increased expression of RORγt, STAT3, IRF4, BATF, and AhR in $CD4^+$ T cells from *PTX3*$^{-/-}$ mice under Th17 polarizing conditions, which correlated with enhanced Th17 and IL-17A responses. The addition of rPTX3 significantly suppressed the expression of RORγt, STAT3, and AhR, transcription factors and IL-17A production. In contrast, the expression of TBX21 and GATA3, key transcription factors for the differentiation of Th1 and Th2 cells, was not affected. These findings show that PTX3 is capable of specifically downregulating these multiple transcription factors to suppress Th17 response. Our findings are in line with a previous study, which showed that the deficiency of PTX3 led to an enhanced Th17 response via the upregulation of STAT3 in a murine model of allergic asthma (Balhara et al., 2017).

Although different inflammatory cytokines (including IL-1β and TNF-α), TLR agonists (e.g., LPS), pathogen-associated molecular patterns (PAMPs), and pathogens have been shown to induce PTX3 expression in cells (Bottazzi et al., 2010; Garlanda et al., 2005; Inforzato et al., 2011; Jaillon et al., 2007), its induction by *Leishmania* has never been reported. We found that *Leishmania* infection induced massive expression of PTX3 by $CD68^+$ cells at the site of infection. Whether this induction is direct (via parasite-derived molecules) or indirect (via production of cytokines by infected cells) remains unknown. Interestingly, we found that the infection of BMDMs with *L. major* resulted in a significant induction of PTX3 mRNA, and this was significantly upregulated by concomitant LPS stimulation (Figure S1). It is conceivable that some parasite-derived molecules such as LPG or GP63 could play a role in the induction of PTX3 following infection to downregulate the protective Th17 response. This could be a novel evasion strategy used by *Leishmania* to subvert the host immune response, thereby favoring its survival within the infected host.

Although our data strongly suggest that the enhanced resistance observed in infected *PTX3*$^{-/-}$ mice is related to strong Th17/IL-17 responses, it is conceivable that other mechanisms may contribute to this phenotype. Infected *PTX3*$^{-/-}$ mice had significantly lower IL-10 responses during the early phase of the infection. However, this difference was not sustained during the chronic phase of the disease. Given that IL-10 has been shown to dampen effector Th1-mediated immunity against *L. major* (Belkaid et al., 2001; Kane and Mosser, 2001; Schwarz et al., 2013), it is plausible that the impaired early IL-10 response in infected *PTX3*$^{-/-}$ mice may permit a more efficient effector Th1 response, leading to more effective parasite control during the chronic phase of the disease. Thus, the lack of studies to unequivocally rule out the impact of this impaired early IL-10 production in the enhanced resistance of *PTX3*$^{-/-}$ mice to *L. major* infection is a major drawback of the present study. In

addition, PTX3 have been shown to bind to apoptotic cells (including neutrophils) and selectively decrease their clearance by immature DCs (Rovere et al., 2000). It is known that *Leishmania* induces early apoptosis in host cells as a means to gain entry into macrophages and DCs (Getti et al., 2008). It is conceivable that the absence of PTX3 in infected *PTX3*$^{-/-}$ mice may lead to the enhanced phagocytosis of parasite-loaded apoptotic neutrophils by DCs, resulting in the increased availability of parasite antigens in these cells. This could result in DC activation and more efficient antigen presentation to T cells leading to enhanced T cell activation and a concomitant enhanced resistance as observed in these mice. Nonetheless, the observation that DCs from *PTX3*$^{-/-}$ mice were more efficient at presenting *L. major*-derived peptides to *Leishmania*-specific TCR transgenic cells leading to IL-17 production *in vitro* suggests that the enhanced uptake of apoptotic neutrophils in the absence of PTX3 may not significantly contribute to the enhanced resistance observed in *PTX3*$^{-/-}$ mice.

The present study reveals a hitherto unknown role of PTX3 in regulating host immunity in CL by suppressing Th17 and IL-17A responses. Following *L. major* infection, the production of PTX3 in WT mice limits the protective IL-17 response by downregulating IL-6 production by DCs and the activation of key transcription factors that favor Th17 activation in CD4$^+$ T cells. In the absence of PTX3 (as seen in *PTX3*$^{-/-}$ mice), increased production of IL-6 and TGF-β by infected DCs favors the optimal differentiation of CD4$^+$T cells into Th17 cells via the increased expression of Th17-specific transcription factors such as STAT3, AhR, and RORγT, leading to the enhanced production of IL-17A. It is conceivable that PTX3 produced by macrophages and DCs may act indirectly (through these cells) to influence Th17 and IL-17A responses. However, we found that highly purified CD4$^+$ T cells from *PTX3*$^{-/-}$ mice differentiated into Th17 cells *in vitro* (in the absence of macrophages or DCs), and this effect was dramatically abolished in a dose-dependent manner by recombinant PTX3 (Figure S7). These observations strongly indicate that PTX3 can directly act on CD4$^+$ T cells and influence their differentiation to IL-17-producing Th17 cells.

Our studies clearly highlight the importance of PTX3 and Th17 cells (and its cytokine, IL-17A) responses in pathogenesis and resistance to CL. The findings that the treatment of WT mice with rPTX3 modulated Th17 response without affecting IFN-γ (Th1) response allowed us to directly demonstrate the contribution of IL-17 in resistance to CL. These findings clearly establish PTX3 as a key innate molecule that negatively regulates Th17 response and IL-17A production and consequently influences optimum resistance to CL. They suggest that PTX3 could be a therapeutic target for modulating immunity and the outcome of the disease.

STAR★METHODS

Detailed methods are provided in the online version of this paper and include the following:

SUPPLEMENTAL INFORMATION

Supplemental Information can be found online at https://doi.org/10.1016/j.celrep.2020.108513.

ACKNOWLEDGMENTS

We thank members of the Uzonna lab for their insightful comments and Dr. Nathan Peters, University of Calgary, Alberta, Canada for supplying *L. braziliensis*. Our research is supported by financial grants from the Canadian Institutes of Health Research (CIHR) and Research Manitoba.

AUTHOR CONTRIBUTIONS

Conceptualization, G.G. and J.E.U.; Investigation, G.G., P.J., R.S., R.Z., S.M.V., L.S., and Z.M.; Writing – Original Draft, G.G. and J.E.U.; Writing – Review & Editing, J.E.U., C.I.d.O., A.S.-G., and T.T.M.; Funding Acquisition, J.E.U.; Resources, J.E.U., C.I.d.O., A.S.-G., T.T.M., A.B., and V.S.B. Supervision, J.E.U.

DECLARATION OF INTERESTS

The authors declare no competing interests.

Received: February 22, 2019
Revised: June 30, 2020
Accepted: November 19, 2020
Published: December 15, 2020

REFERENCES

Abderrahim-Ferkoune, A., Bezy, O., Chiellini, C., Maffei, M., Grimaldi, P., Bonino, F., Moustaid-Moussa, N., Pasqualini, F., Mantovani, A., Ailhaud, G., and Amri, E.Z. (2003). Characterization of the long pentraxin PTX3 as a TNFalpha-induced secreted protein of adipose cells. J. Lipid Res. *44*, 994–1000.

Alvar, J., Vélez, I.D., Bern, C., Herrero, M., Desjeux, P., Cano, J., Jannin, J., and den Boer, M.; WHO Leishmaniasis Control Team (2012). Leishmaniasis worldwide and global estimates of its incidence. PLOS ONE *7*, e35671.

Balhara, J., Shan, L., Zhang, J., Muhuri, A., Halayko, A.J., Almiski, M.S., Doeing, D., McConville, J., Matzuk, M.M., and Gounni, A.S. (2017). Pentraxin 3 deletion aggravates allergic inflammation through a T_H17-dominant phenotype and enhanced CD4 T-cell survival. J. Allergy Clin. Immunol. *139*, 950–963.e9.

Banerjee, A., Bhattacharya, P., Dagur, P.K., Karmakar, S., Ismail, N., Joshi, A.B., Akue, A.D., KuKuruga, M., McCoy, J.P., Jr., Dey, R., and Nakhasi, H.L. (2018). Live Attenuated *Leishmania donovani* Centrin Gene-Deleted Parasites Induce IL-23-Dependent IL-17-Protective Immune Response against Visceral Leishmaniasis in a Murine Model. J. Immunol. *200*, 163–176.

Belkaid, Y., Hoffmann, K.F., Mendez, S., Kamhawi, S., Udey, M.C., Wynn, T.A., and Sacks, D.L. (2001). The role of interleukin (IL)-10 in the persistence of Leishmania major in the skin after healing and the therapeutic potential of anti-IL-10 receptor antibody for sterile cure. J. Exp. Med. *194*, 1497–1506.

Bettelli, E., Carrier, Y., Gao, W., Korn, T., Strom, T.B., Oukka, M., Weiner, H.L., and Kuchroo, V.K. (2006). Reciprocal developmental pathways for the generation of pathogenic effector TH17 and regulatory T cells. Nature *441*, 235–238.

Bittencourt, A.L., Costa, J.M., Carvalho, E.M., and Barral, A. (1993). Leishmaniasis recidiva cutis in American cutaneous leishmaniasis. Int. J. Dermatol. *32*, 802–805.

Bottazzi, B., Doni, A., Garlanda, C., and Mantovani, A. (2010). An integrated view of humoral innate immunity: pentraxins as a paradigm. Annu. Rev. Immunol. *28*, 157–183.

Bozza, S., Bistoni, F., Gaziano, R., Pitzurra, L., Zelante, T., Bonifazi, P., Perruccio, K., Bellocchio, S., Neri, M., Iorio, A.M., et al. (2006). Pentraxin 3 protects from MCMV infection and reactivation through TLR sensing pathways leading to IRF3 activation. Blood *108*, 3387–3396.

Breviario, F., d'Aniello, E.M., Golay, J., Peri, G., Bottazzi, B., Bairoch, A., Saccone, S., Marzella, R., Predazzi, V., Rocchi, M., et al. (1992). Interleukin-1-inducible genes in endothelial cells. Cloning of a new gene related to C-reactive protein and serum amyloid P component. J. Biol. Chem. *267*, 22190–22197.

Brüstle, A., Heink, S., Huber, M., Rosenplänter, C., Stadelmann, C., Yu, P., Arpaia, E., Mak, T.W., Kamradt, T., and Lohoff, M. (2007). The development of inflammatory T(H)-17 cells requires interferon-regulatory factor 4. Nat. Immunol. *8*, 958–966.

Cai, C.W., Blase, J.R., Zhang, X., Eickhoff, C.S., and Hoft, D.F. (2016). Th17 Cells Are More Protective Than Th1 Cells Against the Intracellular Parasite Trypanosoma cruzi. PLOS Pathog. *12*, e1005902.

Carvalho, E.M., Barral, A., Costa, J.M., Bittencourt, A., and Marsden, P. (1994). Clinical and immunopathological aspects of disseminated cutaneous leishmaniasis. Acta Trop. *56*, 315–325.

Ciofani, M., Madar, A., Galan, C., Sellars, M., Mace, K., Pauli, F., Agarwal, A., Huang, W., Parkhurst, C.N., Muratet, M., et al. (2012). A validated regulatory network for Th17 cell specification. Cell *151*, 289–303.

Conti, H.R., Shen, F., Nayyar, N., Stocum, E., Sun, J.N., Lindemann, M.J., Ho, A.W., Hai, J.H., Yu, J.J., Jung, J.W., et al. (2009). Th17 cells and IL-17 receptor signaling are essential for mucosal host defense against oral candidiasis. J. Exp. Med. *206*, 299–311.

D'Angelo, C., De Luca, A., Zelante, T., Bonifazi, P., Moretti, S., Giovannini, G., Iannitti, R.G., Zagarella, S., Bozza, S., Campo, S., et al. (2009). Exogenous pentraxin 3 restores antifungal resistance and restrains inflammation in murine chronic granulomatous disease. J. Immunol. *183*, 4609–4618.

Deban, L., Jaillon, S., Garlanda, C., Bottazzi, B., and Mantovani, A. (2011). Pentraxins in innate immunity: lessons from PTX3. Cell Tissue Res. *343*, 237–249.

Dias, A.A., Goodman, A.R., Dos Santos, J.L., Gomes, R.N., Altmeyer, A., Bozza, P.T., Horta, M.F., Vilcek, J., and Reis, L.F. (2001). TSG-14 transgenic mice have improved survival to endotoxemia and to CLP-induced sepsis. J. Leukoc. Biol. *69*, 928–936.

Dietze-Schwonberg, K., Lopez Kostka, S., Lorenz, B., Regen, T., Waisman, A., and von Stebut, E. (2019). IL-17A/F in Leishmania major-resistant C57BL/6 mice. Exp. Dermatol. *28*, 321–323.

Diniz, S.N., Nomizo, R., Cisalpino, P.S., Teixeira, M.M., Brown, G.D., Mantovani, A., Gordon, S., Reis, L.F., and Dias, A.A. (2004). PTX3 function as an opsonin for the dectin-1-dependent internalization of zymosan by macrophages. J. Leukoc. Biol. *75*, 649–656.

Doni, A., Peri, G., Chieppa, M., Allavena, P., Pasqualini, F., Vago, L., Romani, L., Garlanda, C., and Mantovani, A. (2003). Production of the soluble pattern recognition receptor PTX3 by myeloid, but not plasmacytoid, dendritic cells. Eur. J. Immunol. *33*, 2886–2893.

Doni, A., Garlanda, C., and Mantovani, A. (2016). Innate immunity, hemostasis and matrix remodeling: PTX3 as a link. Semin. Immunol. *28*, 570–577.

dos Santos, C.C., Han, B., Andrade, C.F., Bai, X., Uhlig, S., Hubmayr, R., Tsang, M., Lodyga, M., Keshavjee, S., Slutsky, A.S., and Liu, M. (2004). DNA microarray analysis of gene expression in alveolar epithelial cells in response to TNFalpha, LPS, and cyclic stretch. Physiol. Genomics *19*, 331–342.

Garlanda, C., Hirsch, E., Bozza, S., Salustri, A., De Acetis, M., Nota, R., Maccagno, A., Riva, F., Bottazzi, B., Peri, G., et al. (2002). Non-redundant role of the long pentraxin PTX3 in anti-fungal innate immune response. Nature *420*, 182–186.

Garlanda, C., Bottazzi, B., Bastone, A., and Mantovani, A. (2005). Pentraxins at the crossroads between innate immunity, inflammation, matrix deposition, and female fertility. Annu. Rev. Immunol. *23*, 337–366.

Getti, G.T., Cheke, R.A., and Humber, D.P. (2008). Induction of apoptosis in host cells: a survival mechanism for Leishmania parasites? Parasitology *135*, 1391–1399.

Gonzalez-Lombana, C., Gimblet, C., Bacellar, O., Oliveira, W.W., Passos, S., Carvalho, L.P., Goldschmidt, M., Carvalho, E.M., and Scott, P. (2013). IL-17 mediates immunopathology in the absence of IL-10 following Leishmania major infection. PLOS Pathog. *9*, e1003243.

Goodman, A.R., Levy, D.E., Reis, L.F., and Vilcek, J. (2000). Differential regulation of TSG-14 expression in murine fibroblasts and peritoneal macrophages. J. Leukoc. Biol. *67*, 387–395.

Gupta, G., Oghumu, S., and Satoskar, A.R. (2013). Mechanisms of immune evasion in leishmaniasis. Adv. Appl. Microbiol. *82*, 155–184.

Han, B., Mura, M., Andrade, C.F., Okutani, D., Lodyga, M., dos Santos, C.C., Keshavjee, S., Matthay, M., and Liu, M. (2005). TNFalpha-induced long pentraxin PTX3 expression in human lung epithelial cells via JNK. J. Immunol. *175*, 8303–8311.

Inforzato, A., Jaillon, S., Moalli, F., Barbati, E., Bonavita, E., Bottazzi, B., Mantovani, A., and Garlanda, C. (2011). The long pentraxin PTX3 at the crossroads between innate immunity and tissue remodelling. Tissue Antigens *77*, 271–282.

Introna, M., Alles, V.V., Castellano, M., Picardi, G., De Gioia, L., Bottazzai, B., Peri, G., Breviario, F., Salmona, M., De Gregorio, L., et al. (1996). Cloning of mouse ptx3, a new member of the pentraxin gene family expressed at extrahepatic sites. Blood *87*, 1862–1872.

Ivanov, I.I., McKenzie, B.S., Zhou, L., Tadokoro, C.E., Lepelley, A., Lafaille, J.J., Cua, D.J., and Littman, D.R. (2006). The orphan nuclear receptor RORgammat directs the differentiation program of proinflammatory IL-17+ T helper cells. Cell *126*, 1121–1133.

Jaillon, S., Peri, G., Delneste, Y., Frémaux, I., Doni, A., Moalli, F., Garlanda, C., Romani, L., Gascan, H., Bellocchio, S., et al. (2007). The humoral pattern recognition receptor PTX3 is stored in neutrophil granules and localizes in extracellular traps. J. Exp. Med. *204*, 793–804.

Jeannin, P., Bottazzi, B., Sironi, M., Doni, A., Rusnati, M., Presta, M., Maina, V., Magistrelli, G., Haeuw, J.F., Hoeffel, G., et al. (2005). Complexity and complementarity of outer membrane protein A recognition by cellular and humoral innate immunity receptors. Immunity *22*, 551–560.

Kane, M.M., and Mosser, D.M. (2001). The role of IL-10 in promoting disease progression in leishmaniasis. J. Immunol. *166*, 1141–1147.

Kolls, J.K., and Lindén, A. (2004). Interleukin-17 family members and inflammation. Immunity *21*, 467–476.

Launois, P., Maillard, I., Pingel, S., Swihart, K.G., Xénarios, I., Acha-Orbea, H., Diggelmann, H., Locksley, R.M., MacDonald, H.R., and Louis, J.A. (1997). IL-4 rapidly produced by V beta 4 V alpha 8 CD4+ T cells instructs Th2 development and susceptibility to Leishmania major in BALB/c mice. Immunity *6*, 541–549.

Liu, D., and Uzonna, J.E. (2010). The p110 delta isoform of phosphatidylinositol 3-kinase controls the quality of secondary anti-Leishmania immunity by regulating expansion and effector function of memory T cell subsets. J. Immunol. *184*, 3098–3105.

Liu, D., Zhang, T., Marshall, A.J., Okkenhaug, K., Vanhaesebroeck, B., and Uzonna, J.E. (2009). The p110delta isoform of phosphatidylinositol 3-kinase controls susceptibility to Leishmania major by regulating expansion and tissue homing of regulatory T cells. J. Immunol. *183*, 1921–1933.

Liu, X., Hu, H., Fan, H., Zuo, D., Shou, Z., Liao, Y., Nan, Z., and Tang, Q. (2017). The role of STAT3 and AhR in the differentiation of CD4+ T cells into Th17 and Treg cells. Medicine (Baltimore) *96*, e6615.

Locksley, R.M., Heinzel, F.P., Holaday, B.J., Mutha, S.S., Reiner, S.L., and Sadick, M.D. (1991). Induction of Th1 and Th2 CD4+ subsets during murine Leishmania major infection. Res. Immunol. *142*, 28–32.

Locksley, R.M., Reiner, S.L., Hatam, F., Littman, D.R., and Killeen, N. (1993). Helper T cells without CD4: control of leishmaniasis in CD4-deficient mice. Science *261*, 1448–1451.

Lopez Kostka, S., Dinges, S., Griewank, K., Iwakura, Y., Udey, M.C., and von Stebut, E. (2009). IL-17 promotes progression of cutaneous leishmaniasis in susceptible mice. J. Immunol. *182*, 3039–3046.

Ma, Y.J., Doni, A., Hummelshøj, T., Honoré, C., Bastone, A., Mantovani, A., Thielens, N.M., and Garred, P. (2009). Synergy between ficolin-2 and pentraxin 3 boosts innate immune recognition and complement deposition. J. Biol. Chem. *284*, 28263–28275.

Mengesha, B.G., and Conti, H.R. (2017). The Role of IL-17 in Protection against Mucosal Candida Infections. J. Fungi (Basel) *3*, E52.

Merad, M., Sathe, P., Helft, J., Miller, J., and Mortha, A. (2013). The dendritic cell lineage: ontogeny and function of dendritic cells and their subsets in the steady state and the inflamed setting. Annu. Rev. Immunol. *31*, 563–604.

Moalli, F., Doni, A., Deban, L., Zelante, T., Zagarella, S., Bottazzi, B., Romani, L., Mantovani, A., and Garlanda, C. (2010). Role of complement and Fcgamma receptors in the protective activity of the long pentraxin PTX3 against Aspergillus fumigatus. Blood *116*, 5170–5180.

Moalli, F., Paroni, M., Véliz Rodriguez, T., Riva, F., Polentarutti, N., Bottazzi, B., Valentino, S., Mantero, S., Nebuloni, M., Mantovani, A., et al. (2011). The therapeutic potential of the humoral pattern recognition molecule PTX3 in chronic lung infection caused by Pseudomonas aeruginosa. J. Immunol. *186*, 5425–5434.

Mou, Z., Li, J., Boussoffara, T., Kishi, H., Hamana, H., Ezzati, P., Hu, C., Yi, W., Liu, D., Khadem, F., et al. (2015). Identification of broadly conserved cross-species protective Leishmania antigen and its responding CD4+ T cells. Sci. Transl. Med. *7*, 310ra167.

Nascimento, M.S., Carregaro, V., Lima-Júnior, D.S., Costa, D.L., Ryffel, B., Duthie, M.S., de Jesus, A., de Almeida, R.P., and da Silva, J.S. (2015). Interleukin 17A acts synergistically with interferon γ to promote protection against Leishmania infantum infection. J. Infect. Dis. *211*, 1015–1026.

Novoa, R., Bacellar, O., Nascimento, M., Cardoso, T.M., Ramasawmy, R., Oliveira, W.N., Schriefer, A., and Carvalho, E.M. (2011). IL-17 and Regulatory Cytokines (IL-10 and IL-27) in L. braziliensis Infection. Parasite Immunol. *33*, 132–136.

Oghumu, S., Gupta, G., Snider, H.M., Varikuti, S., Terrazas, C.A., Papenfuss, T.L., Kaplan, M.H., and Satoskar, A.R. (2014). STAT4 is critical for immunity but not for antileishmanial activity of antimonials in experimental visceral leishmaniasis. Eur. J. Immunol. *44*, 450–459.

Okwor, I., Xu, G., Tang, H., Liang, Y., Fu, Y.X., and Uzonna, J.E. (2015). Deficiency of CD40 Reveals an Important Role for LIGHT in Anti-Leishmania Immunity. J. Immunol. *195*, 194–202.

Pedraza-Zamora, C.P., Delgado-Domínguez, J., Zamora-Chimal, J., and Becker, I. (2017). Th17 cells and neutrophils: Close collaborators in chronic Leishmania mexicana infections leading to disease severity. Parasite Immunol. *39*. https://doi.org/10.1111/pim.12420.

Pitta, M.G., Romano, A., Cabantous, S., Henri, S., Hammad, A., Kouriba, B., Argiro, L., el Kheir, M., Bucheton, B., Mary, C., et al. (2009). IL-17 and IL-22 are associated with protection against human kala azar caused by Leishmania donovani. J. Clin. Invest. *119*, 2379–2387.

Priebe, G.P., Walsh, R.L., Cederroth, T.A., Kamei, A., Coutinho-Sledge, Y.S., Goldberg, J.B., and Pier, G.B. (2008). IL-17 is a critical component of vaccine-induced protection against lung infection by lipopolysaccharide-heterologous strains of Pseudomonas aeruginosa. J. Immunol. *181*, 4965–4975.

Quintana, F.J., Basso, A.S., Iglesias, A.H., Korn, T., Farez, M.F., Bettelli, E., Caccamo, M., Oukka, M., and Weiner, H.L. (2008). Control of T(reg) and T(H)17 cell differentiation by the aryl hydrocarbon receptor. Nature *453*, 65–71.

Reading, P.C., Bozza, S., Gilbertson, B., Tate, M., Moretti, S., Job, E.R., Crouch, E.C., Brooks, A.G., Brown, L.E., Bottazzi, B., et al. (2008). Antiviral activity of the long chain pentraxin PTX3 against influenza viruses. J. Immunol. *180*, 3391–3398.

Reiner, S.L., and Locksley, R.M. (1995). The regulation of immunity to Leishmania major. Annu. Rev. Immunol. *13*, 151–177.

Rovere, P., Peri, G., Fazzini, F., Bottazzi, B., Doni, A., Bondanza, A., Zimmermann, V.S., Garlanda, C., Fascio, U., Sabbadini, M.G., et al. (2000). The long pentraxin PTX3 binds to apoptotic cells and regulates their clearance by antigen-presenting dendritic cells. Blood *96*, 4300–4306.

Salio, M., Chimenti, S., De Angelis, N., Molla, F., Maina, V., Nebuloni, M., Pasqualini, F., Latini, R., Garlanda, C., and Mantovani, A. (2008). Cardioprotective function of the long pentraxin PTX3 in acute myocardial infarction. Circulation *117*, 1055–1064.

Schraml, B.U., Hildner, K., Ise, W., Lee, W.L., Smith, W.A., Solomon, B., Sahota, G., Sim, J., Mukasa, R., Cemerski, S., et al. (2009). The AP-1 transcription factor Batf controls T(H)17 differentiation. Nature *460*, 405–409.

Schwarz, T., Remer, K.A., Nahrendorf, W., Masic, A., Siewe, L., Müller, W., Roers, A., and Moll, H. (2013). T cell-derived IL-10 determines leishmaniasis disease outcome and is suppressed by a dendritic cell based vaccine. PLOS Pathog. *9*, e1003476.

Scott, P. (1996). Th cell development and regulation in experimental cutaneous leishmaniasis. Chem. Immunol. *63*, 98–114.

Sheel, M., Beattie, L., Frame, T.C., de Labastida Rivera, F., Faleiro, R.J., Bunn, P.T., Montes de Oca, M., Edwards, C.L., Ng, S.S., Kumar, R., et al. (2015). IL-17A-Producing $\gamma\delta$ T Cells Suppress Early Control of Parasite Growth by Monocytes in the Liver. J. Immunol. *195*, 5707–5717.

Sia, J.K., Georgieva, M., and Rengarajan, J. (2015). Innate Immune Defenses in Human Tuberculosis: An Overview of the Interactions between Mycobacterium tuberculosis and Innate Immune Cells. J. Immunol. Res. *2015*, 747543.

Soares, A.C., Souza, D.G., Pinho, V., Vieira, A.T., Nicoli, J.R., Cunha, F.Q., Mantovani, A., Reis, L.F., Dias, A.A., and Teixeira, M.M. (2006). Dual function of the long pentraxin PTX3 in resistance against pulmonary infection with Klebsiella pneumoniae in transgenic mice. Microbes Infect. *8*, 1321–1329.

Souza, D.G., Amaral, F.A., Fagundes, C.T., Coelho, F.M., Arantes, R.M., Sousa, L.P., Matzuk, M.M., Garlanda, C., Mantovani, A., Dias, A.A., and Teixeira, M.M. (2009). The long pentraxin PTX3 is crucial for tissue inflammation after intestinal ischemia and reperfusion in mice. Am. J. Pathol. *174*, 1309–1318.

Srivastava, S., Ernst, J.D., and Desvignes, L. (2014). Beyond macrophages: the diversity of mononuclear cells in tuberculosis. Immunol. Rev. *262*, 179–192.

Terrazas, C., Varikuti, S., Kimble, J., Moretti, E., Boyaka, P.N., and Satoskar, A.R. (2016). IL-17A promotes susceptibility during experimental visceral leishmaniasis caused by Leishmania donovani. FASEB J. *30*, 1135–1143.

Turetz, M.L., Machado, P.R., Ko, A.I., Alves, F., Bittencourt, A., Almeida, R.P., Mobashery, N., Johnson, W.D., Jr., and Carvalho, E.M. (2002). Disseminated leishmaniasis: a new and emerging form of leishmaniasis observed in northeastern Brazil. J. Infect. Dis. *186*, 1829–1834.

Uzonna, J.E., Joyce, K.L., and Scott, P. (2004). Low dose Leishmania major promotes a transient T helper cell type 2 response that is down-regulated by interferon gamma-producing CD8+ T cells. J. Exp. Med. *199*, 1559–1566.

Xu, G., Liu, D., Okwor, I., Wang, Y., Korner, H., Kung, S.K., Fu, Y.X., and Uzonna, J.E. (2007). LIGHT Is critical for IL-12 production by dendritic cells, optimal CD4+ Th1 cell response, and resistance to Leishmania major. J. Immunol. *179*, 6901–6909.

Yang, X.O., Panopoulos, A.D., Nurieva, R., Chang, S.H., Wang, D., Watowich, S.S., and Dong, C. (2007). STAT3 regulates cytokine-mediated generation of inflammatory helper T cells. J. Biol. Chem. *282*, 9358–9363.

Zhang, J., Koussih, L., Shan, L., Halayko, A.J., Chen, B.K., and Gounni, A.S. (2015). TNF up-regulates Pentraxin3 expression in human airway smooth muscle cells via JNK and ERK1/2 MAPK pathways. Allergy Asthma Clin. Immunol. *11*, 37.

STAR★METHODS

KEY RESOURCES TABLE

REAGENT or RESOURCE	SOURCE	IDENTIFIER
Antibodies		
Mouse Anti IL-17A (Clone 17F3mAb)	Bioxcell	Catalog # BE0173
Mouse anti IgG1 isotype control (Clone MOPC-21)	Bioxcell	Catalog # BE0083
Mouse anti IL-4 Antibody (Clone 11B11)	Biolegend	Catalog # 504121
Mouse anti CD3 Antibody (Clone 145-2C11)	Biolegend	Catalog # 100339
Mouse CD28 Antibody (Clone 28.2)	Biolegend	Catalog # 302933
Mouse IL-2 Antibody (Clone JES6-1A12)	Biolegend	Catalog # 503702
Mouse IFN-γ Antibody (Clone XMG1.2)	Biolegend	Catalog # 505802
Mouse IL-12 Antibody (Clone C17.8)	Biolegend	Catalog # 505307
FITC anti-mouse CD19 Antibody (Clone 1D3/CD19)	Biolegend	Catalog # 152404
APC anti-mouse CD4 Antibody (Clone GK1.5)	Biolegend	Catalog # 100412
PE-Cy7 anti-mouse CD4 Antibody (Clone GK1.5)	Biolegend	Catalog # 100421
APC-Cy7 anti-mouse CD4 Antibody (Clone GK1.5)	Biolegend	Catalog # 100413
Alexa fluor 488 anti-mouse CD4 Antibody (Clone GK1.5)	Biolegend	Catalog # 100425
Pacific Blue anti-mouse CD4 Antibody (Clone GK1.5)	Biolegend	Catalog # 100428
Pacific Blue anti-mouse CD90.2 Antibody (Clone 53-2.1)	Biolegend	Catalog # 140306
Alexa Fluor® 488 anti-mouse CD90.2 Antibody (Clone 30-H12)	Biolegend	Catalog # 105316
APC-Cy7 anti-mouse CD3 Antibody (Clone 145-2C11)	Biolegend	Catalog # 100329
PE-Cy7 anti-mouse CD3 Antibody (Clone 145-2C11)	Biolegend	Catalog # 100319
Pacific Blue anti-mouse CD3 Antibody (Clone 145-2C11)	Biolegend	Catalog # 100333
PE anti-mouse Ly-6G/Ly-6C (Gr-1) Antibody (Clone RB6-8C5)	Biolegend	Catalog # 108408
FITC anti-mouse Ly-6C Antibody (Clone HK1.4)	Biolegend	Catalog # 128005
APC anti-mouse/human CD11b Antibody (Clone M1/70)	Biolegend	Catalog # 101211
Pacific Blue anti-mouse/human CD11b Antibody (Clone M1/70)	Biolegend	Catalog # 101223
Pacific Blue anti-mouse Ly6G Antibody (Clone 1A8)	Biolegend	Catalog # 127611
PE anti-mouse CD11c Antibody (Clone N418)	Biolegend	Catalog # 117307
Pacific Blue anti-mouse IA/IE Antibody (Clone M5/114.15.2)	Biolegend	Catalog # 107619
APC anti-mouse TNF alpha Antibody (Clone MP6-XT22)	Biolegend	Catalog # 506307
APC anti-mouse IL-6 Antibody (Clone MP5-20F3)	Biolegend	Catalog # 504507
PerCP/Cy5.5 anti-mouse IL-10 Antibody (Clone JES5-16E3)	Biolegend	Catalog # 505027
APC anti-mouse IL-6 Antibody (Clone TC11-18H10.1)	Biolegend	Catalog # 506915
APC anti-mouse CD25 Antibody (Clone 3C7)	Biolegend	Catalog # 101909
PE anti-mouse FOXP3 Antibody (Clone MF-14)	Biolegend	Catalog # 126403
PerCP Cy5.5 anti-mouse IFN-γ Antibody (Clone XMG1.2)	Biolegend	Catalog # 505801
Human/mouse Anti-PTX3 Antibody (Clone MNB1)	Enzo Lifesciences	Catalog # 1ALX-804-463-C100
Mouse Anti-CD68 Antibody	Abcam	Catalog # ab125212
Alexa fluor 568 Goat Anti-rat Antibody	Invitrogen	Catalog # A-11077
Alexa fluor 568 Goat Anti-rabbit Antibody	Invitrogen	Catalog # A27040
Chemicals, Peptides, and Recombinant Proteins		
Recombinant Mouse IFN-γ (carrier-free)	Biolegend	Catalog # 575306
Recombinant Mouse TGF-β1 (carrier-free)	Biolegend	Catalog # 763104
Recombinant Mouse IL-12p70 (carrier-free)	Biolegend	Catalog # 577004

(*Continued on next page*)

Continued

REAGENT or RESOURCE	SOURCE	IDENTIFIER
Recombinant Mouse IL-6 (carrier-free)	Biolegend	Catalog # 575704
Recombinant Mouse IL-17A Protein (carrier-free)	R&D Systems	Catalog # 421-ML-025/CF
Recombinant Mouse Pentraxin 3/TSG-14 Protein (carrier-free)	R&D Systems	Catalog # 2166-TS-025/CF
Recombinant Mouse GM CSF Protein (carrier-free)	R&D Systems	Catalog # 415-ML-01M/CF
Recombinant Mouse M-CSF Protein (carrier-free)	R&D Systems	Catalog # 416-ML-050/CF
Fc Receptor Blocker	Innovex	Catalog # NB309-15
Hoechst 33342	Molecular Probes/invitrogen	Catalog # H3570
ProLong Gold Antifade Mountant	Invitrogen	Catalog # P10144
Tissue Plus OCT compound	Fischer Scientific	Catalog# 23-730-571
DNase I	QIAGEN	Catalog# EN0521
Saponin	Sigma	Catalog# SAE0073-10G
5(6)-Carboxyfluorescein diacetate *N*-succinimidyl ester	Sigma	Catalog # 21888-25MG-F
PEPCK peptide: NDAFGVMPPVARLTPEQ	SelleckChem	Not Available
Critical Commercial Assays		
Mouse Regulatory T Cell Staining Kit	eBioscience	Catalog # 88-8111-40
ELISA MAX Standard Set Mouse IL-17A	Biolegend	Catalog # 432501
ELISA MAX Standard Set Mouse IL-10	Biolegend	Catalog # 431411
ELISA MAX Standard Set Mouse IFN-γ	Biolegend	Catalog # 431411
Mouse IFN-γ ELISA Kit	BD OptEIA	Catalog # 558258
High-Capacity RNA-to-cDNA Kit	Applied Biosystems	Catalog # 4387406
EasySep Mouse CD11c Positive Selection Kit	StemCell Technologies, Inc.	Catalog #18780RF
EasySep Mouse Memory CD4+ T Cell Isolation Kit	StemCell Technologies, Inc.	Catalog #19767
RNeasy Plus Micro Kit. mRNA	QIAGEN	Catalog # 74034
RNeasy Mini Kit	QIAGEN	Catalog # 74104
PowerUp SYBR Green Master Mix	Applied Biosystems	Catalog # A25743
TaqMan Gene Expression assay for human PTX3	Applied Biosystems	Catalog # Hs00173615_m1
TaqMan Gene Expression assay for human IL-17A	Applied Biosystems	Catalog # Hs00174383_m1
TaqMan Gene Expression assay for human GAPDH	Applied Biosystems	Catalog # Hs03929097_g1
Experimental Models: Cell Lines		
Leishmania major [MHOM/IL/80/Friedlin (FN)]	Liu et al., 2009	Not available
Leishmania. braziliensis (Human isolate)	Dr Nathan Peters	Not available
Experimental Models: Organisms/Strains		
Mouse: C57BL/6 (Wild Type)	University of Manitoba Central Animal Care Services	N/A
Mouse: Heterozygous PTX3$^{+/-}$ on C57BL6 background	University of Manitoba Central Animal Care Services	N/A
Mouse: Homozygous PTX3$^{+/+}$ on C57BL6 background	University of Manitoba Central Animal Care Services	N/A
Mouse: PEPCK TCR-transgenic C57BL6	University of Manitoba Central Animal Care Services	N/A
Oligonucleotides		
Mouse Forward PTX3-CCTGCGATCCTGCTTTGTG	Primer Bank	ID: 31982085a1
Mouse Reverse PTX3-GGTGGGATGAAGTCCATTGTC	Primer Bank	ID: 31982085a1
Mouse Forward GAPDH-AGGTCGGTGTGAACGGATTTG	Primer Bank	ID: 6679937a1
Mouse Reverse GAPDH-TGTAGACCATGTAGTTGAGGTCA	Primer Bank	ID: 6679937a1
Mouse Forward IL-17A-TTTAACTCCCTTGGCGCAAAA	Primer Bank	ID: 6754324a1
Mouse Reverse IL-17A-CTTTCCCTCCGCATTGACAC	Primer Bank	ID: 6754324a1
Mouse Forward iNOS2: GTTCTCAGCCCAACAATACAAGA	Primer Bank	ID: 6754872a1
Mouse Reverse iNOS2-GTGGACGGGTCGATGTCAC	Primer Bank	ID: 6754872a1

(*Continued on next page*)

Continued

REAGENT or RESOURCE	SOURCE	IDENTIFIER
Mouse Forward RoRγ: GACCCACACCTCACAAATTGA	Primer Bank	ID: 6755344a1
Mouse Reverse RoRγ: - AGTAGGCCACATTACACTGCT	Primer Bank	ID: 6755344a1
Mouse Forward TBX21: AGCAAGGACGGCGAATGTT	Primer Bank	ID: 9507179a1
Mouse Reverse TBX21: GGGTGGACATATAAGCGGTTC	Primer Bank	ID: 9507179a1
Mouse Forward GATA3: CTCGGCCATTCGTACATGGAA	Primer Bank	ID: 6679951a1
Mouse Reverse GATA3: GGATACCTCTGCACCGTAGC	Primer Bank	ID: 6679951a1
Mouse Forward BATF: CTGGCAAACAGGACTCATCTG	Primer Bank	ID: 7949007a1
Mouse Reverse BATF: GGGTGTCGGCTTTCTGTGTC	Primer Bank	ID: 7949007a1
Mouse Forward AhR: CTGGCAAACAGGACTCATCTG	Primer Bank	ID: 19526637a1
Mouse Reverse AhR: AGGCGGTCTAACTCTGTGTTC	Primer Bank	ID: 19526637a1
Mouse Forward STAT3:CAATACCATTGACCTGCCGAT	Primer Bank	ID: 13277852a1
Mouse Reverse STAT3: GAGCGACTCAAACTGCCCT	Primer Bank	ID: 13277852a1
Mouse Forward IRF4: TCCGACAGTGGTTGATCGAC	Primer Bank	ID: 7305519a1
Mouse Reverse IRF4: CCTCACGATTGTAGTCCTGCTT	Primer Bank	ID: 7305519a1
Software and Algorithms		
FlowJo 10 Software	FlowJO, LLC	https://www.flowjo.com/solutions/flowjo/downloads
ImageJ.exe 1.52a Software	NIH	https://imagej.nih.gov/ij/download.html
Prism 6 Software	GraphPad Prism	https://www.graphpad.com/scientific-software/prism
EndNote Web	Web of Science Group	https://endnote.com
Other		
M199 Medium	Hyclone	Cat # SH30253.02
DMEM Medium	GIBCO	Cat # 12430112
Heat Inactivated Fetal Bovine Serum	Hyclone	Cat # SH30071.03IH30-45
Penicillin/Streptomycin	Invitrogen	Cat # 15140122
Cell Staining Buffer	Biolegend	Cat # 420201
ACK Lysing solution Buffer	GIBCO	Cat # A10492-01

RESOURCE AVAILABILITY

Lead Contact

Further information and requests regarding resources and reagents should be directed to and will be fulfilled by the Lead Contact, Jude E Uzonna (jude.uzonna@umanitoba.ca).

Materials Availability

This study did not generate new unique reagents or mouse lines.

Data and Code Availability

This study did not generate any unique datasets or code. No custom code was used to analyze these data and all methods used are cited in the STAR Methods section.

EXPERIMENTAL MODEL AND SUBJECT DETAILS

Mice

Heterozygous female *PTX3*$^{+/-}$ and homozygous male *PTX3*$^{-/-}$ (originally on129SvEv/Bl/6 background and backcrossed for over 10 generations unto C57BL/6 background) mice were bred at the University of Manitoba Central Animal Care Services (CACS) breeding facility. Female homozygous PTX3 deficient (*PTX3*$^{-/-}$), heterozygous (*PTX3*$^{+/-}$) and their homozygous C57BL/6 (wild-type, WT) control mice (6-8 weeks old) were used in the studies. Female PEPCK TCR-transgenic mice on the C57BL/6 genetic background were

developed and generated by us as described below and bred at the CACS. All $CD4^+$ T cells from these mice recognize a highly conserved and immunodominant $PEPCK_{335-351}$ peptide derived from *L. major* phosphoenolpyruvate carboxylkinase (PEPCK) protein (Mou et al., 2015). All animal studies were approved by the University of Manitoba Animal Care Committee in accordance with the Canadian Council for Animal Care guidelines.

Generation of PEPCK-specific TCR Transgenic mice

PEPCK-specific $CD4^+$ T cells were isolated (by cell sorting) from spleens of *L. major*-infected C57BL/6 mice following staining with $I\text{-}A^b\text{-}PEPCK_{335-351}$ tetramer (Mou et al., 2015). The TCR beta and alpha genes were amplified from tetramer binding cells by single-cell RT-PCR as previously described (Mou et al., 2015). The TCRβ-P2A-TCRα cDNA was subcloned into VA hCD2 transgenic cassette vector. Linearized transgenic plasmid DNA fragments were injected into the pronuclei of fertilized C57BL/6 eggs and the resulting embryos were implanted into surrogate mothers to obtain offspring. Founders and their progeny were screened by assessing peripheral blood mononuclear cells for transgene TCR expression by flow cytometry using $I\text{-}A^b\text{-}PEPCK_{335-351}$ tetramer.

Human CL patients and ethical statement

This study was conducted in Jequiriça, Bahia, Brazil, a well-known area of *L. braziliensis* transmission. Participants included 3 healthy endemic controls and 17 patients with Tegumentary leishmaniasis with cutaneous lesions typical of *Leishmania* infection and a positive Montenegro skin test (Table S1). This research was conducted with the approval of the Ethical Committee of Hospital Santa Izabel-Santa Casa de Misericórdia da Bahia (Salvador, Bahia, Brazil; 1.163.870) and Comissão Nacional de Éticaem Pesquisa (CEP, Brazilian National Ethics Committee, Brazil). Informed consent was obtained from each participant. All methods were performed in accordance with the guidelines and regulations determined by CEP.

Parasites and infection

L. major parasites [MHOM/IL/80/Friedlin (FN)] and *L. braziliensis* (human isolate obtained from Dr. Nathan Peters, University of Calgary, Canada) were cultured at 26°C in M199 medium (HyClone, Logan, UT) supplemented with 20% heat-inactivated FBS (HyClone), 2 mM L-glutamine, 100 U/mL penicillin, and 100 μg/mL streptomycin (Invitrogen Life Technologies, Burlington, Ontario, Canada). For infection, mice were injected in the right hind footpad with 2×10^6 stationary phase promastigotes in 50 μL PBS as previously described (Liu et al., 2009). In some experiments, the mice were injected intradermally in the ear with 2×10^6 (*L. major*), 1×10^6 (*L. braziliensis*) stationary phase promastigotes or 1×10^3 *L. major* purified (by negative PNA agglutination) metacyclic promastigotes in 10 μL PBS. Lesion sizes were monitored weekly by measuring footpad swellings with digital calipers. Parasite burden in the infected footpads and ears was determined by limiting dilution assay.

METHOD DETAILS

In vivo blockade of IL-17A, rPTX3 treatment and estimation of parasite burden

For *in vivo* neutralization of IL-17A, WT and $PTX3^{-/-}$ mice were injected with anti–IL-17A (clone 17F3) mAb or control Ig (1 mg/mouse) i.p.1 day before infection with *L. major*. Antibody treatment was continued once weekly at 0.5 mg/mouse for additional 4 weeks. The lesion thickness was monitored weekly and mice were sacrificed after 4 weeks post infection to determine parasite burden. To assess the impact of PTX3 on disease outcome, infected WT mice were either injected locally (intraleisonally) with PBS or rPTX3 (0.5 mg in 50 μL PBS) thrice weekly and lesion thickness was monitored weekly. Treated mice were sacrificed at 4 weeks post-infection to determine immune response in spleens and dLNs and parasite burden in the infected footpads. Parasite burden in the infected footpads was quantified by limiting dilution analysis as previously described (Uzonna et al., 2004).

In vitro recall response and intracellular cytokine staining

At various times post-infection, infected mice were sacrificed and the draining popliteal lymph nodes or cervical lymph nodes (ear infection) were harvested and made into single-cell suspensions. Cells were washed, resuspended at 4 million/ml in complete medium (DMEM supplemented with 10% heat-inactivated FBS, 2 mM glutamine, 100 U/ml penicillin, and 100 μg/ml streptomycin), and plated at 1 ml/well in 24-well tissue culture plate (Falcon, VWR Edmonton, AB, Canada). Cells were stimulated with SLA (50 μg/ml) for 72 h, and the supernatant fluids were collected and stored at −20°C until assayed for cytokines by ELISA.

Cytokine ELISAs and NO

IL-17A, IFN-γ and IL-10 concentrations in cell culture supernatant fluids were measured by sandwich ELISA using Ab pairs from BD PharMingen or Biolegend according to manufacturer's suggested protocols. Nitrite concentrations in BMDM culture supernatants were used as a measure of NO production and quantified using the Griess assay.

Generation of BMDMs, BMDCs and *in vitro* infections

BMDCs and BMDMs were generated from naive WT and $PTX3^{-/-}$ mice as described previously (Liu et al., 2009). In brief, bone marrow cells were isolated from the femur and tibia of mice and differentiated into macrophages using complete medium supplemented with 30% L929 cell culture supernatant. For BMDC differentiation, the bone marrow cells were grown using complete me-

dium supplemented with 20ng/mL GM-CSF. For infection, BMDCs or BMDMs were incubated with parasites for 3h or 6h at a cell/parasite ratio of 1:10 as previously described (Liu et al., 2009). In some experiments, infected cells were stimulated with IFN-γ (100 and 10 ng/mL), IL-17A (100 and 50 ng/mL) and LPS (1 μg/mL). At different times after infection, parasite numbers inside infected cells were determined by counting Giemsa stained cytospin preparations under light microscope at 100x (oil) objective. In addition, the culture supernatant fluids were also assessed for nitrite concentration. In some experiments, BMDCs were stimulated *in vitro* with LPS (1 μg/mL) for 24 h, and culture supernatant fluids were assayed for TGF-β, IL-12p40 and IL-6 by ELISA.

Purification of splenic CD4$^+$ T cells and CD11c$^+$ (dendritic) cells

Splenic CD4$^+$ T and CD11c$^+$ cells were isolated by negative and positive selection using the StemCell CD4$^+$ T and CD11c$^+$ cells Easy-Sep isolation kits, respectively, according to the manufacturer's suggested protocols. The purities of the different cell populations were > 94% (CD4$^+$) and 87–93% (CD11c$^+$).

In vitro Th1 and Th17 differentiation

Single-cell suspensions from the spleens (whole splenocytes) or highly purified naive CD4$^+$ (CD44$^-$CD62$^+$) cells from WT and KO mice were labeled with CFSE dye as previously described (Liu and Uzonna, 2010) and cultured in 96-well plates (2×10^5 per well in 200 μL aliquots) in the presence of plate-bound anti-CD3 (1 μg/mL) and anti-CD28 (1 μg/mL) under varying polarizing conditions as follows: Th1, rIL-12 (20 ng/mL) and anti-IL-4 (10 μg/mL); Th17, rTGF-β (10 ng/mL), rIL-6 (100 ng/mL), anti-IL-4 (10 μg/mL), anti-IL-2 (10 μg/mL) anti-IFN-γ (10 μg/mL), and anti-IL-12 (10 μg/mL). All recombinant cytokines and endotoxin-free mAbs were purchased either from R&D Systems or BioLegend (San Diego, CA). In some experiments, rPTX3 (R&D system) was added into the cell cultures. After 5 days of culture, the cells were routinely assessed for proliferation and cytokine production by flow cytometry as described below.

BMDC-T cells Co-culture assays

CFSE labeled highly purified naive CD4$^+$ T cells from PEPCKTCR transgenic mice were cultured for 4 days in 96-well plates with LPS-matured BMDCs from WT and *PTX3*$^{-/-}$ mice at 10:1 (DC to T cell ratio) in presence of PEPCK peptide (5 μM NDAFGVMPPVARLT-PEQ, (Mou et al., 2015) and/or Th17-polarizing cocktail (as described earlier). After 5 days of culture, the cells were routinely assessed for proliferation and cytokine production by flow cytometry as described below.

CFSE labeling and proliferation protocol

The CFSE labeling protocol used here has been described previously (Liu and Uzonna, 2010). Briefly, single-cell suspensions from the spleens or dLNs were counted and stained with CFSE dye at 1.25 μM at room temperature in the dark with continuous rocking. After 5 min, staining was quenched with heat-inactivated FBS and the cells were washed, counted, resuspended in complete medium, and used for *in vitro* cultures.

Quantification of transcript levels by RT-PCR

Total RNA was extracted from murine ear, splenocytes, BMDM, BMDC or purified CD4 T cells using the RNeasy Plus Micro Kit. mRNA was reverse transcribed and cDNA was amplified by RT-PCR using SYBR Green chemistry as described previously (Oghumu et al., 2014). Murine primers and reaction conditions were obtained from the PRIMER BANK website https://pga.mgh.harvard.edu/primerbank (Massachusetts General Hospital Primer Bank). Data were normalized to the housekeeping gene β-actin and presented as fold induction over non-polarized splenocytes or CD4$^+$ T cells using the delta-delta CT method.

Cryopreserved human skin biopsies from lesions of infected or uninfected people were processed into fine powder using the traditional mortar and pestle system. Total RNA was extracted from these samples using RNeasy mini kit (QIAGEN, Venlo, Netherlands) and DNA clean up was performed on-column by DNase treatment (QIAGEN). mRNA was reverse transcribed and cDNA was amplified using Taqman gene expression assays (Applied Biosystems) for PTX3 (Hs00173615_m1), IL17A (Hs00174383_m1) and GAPDH (Hs03929097_g1). All reactions were performed using the standard cycling conditions (Applied Biosystems, Warrington, United Kingdom). Data were normalized to the housekeeping gene GAPDH and presented as fold induction over normal skin (NS) using the delta-delta CT method.

Flow cytometry analysis

For flow cytometry analysis, single cell suspension from spleens, dLNs and ear tissues were stained directly *ex vivo* for CD19, CD4, CD90, GR1, LY6C, Ly6G, CD11b, CD3, CD4, MHC-II and CD11c expression. For intracellular cytokine analysis, surfaced-stained splenocytes and dLN cells were permeabilized with 0.1% saponin (Sigma-Aldrich) in staining buffer and then stained with specific fluorochrome-conjugated mAbs against TNF-α, IL-6, IFN-γ, IL-10 and IL-17 (BioLegend). Samples were acquired on a BD FACSCantor machine and analyzed using FlowJo software (TreeStar Inc, Ashland, OR).

Ex vivo Treg staining

In some experiments, single cell suspensions of spleens and dLN cells were directly stained *ex vivo* for surface expression of CD3, CD4 and CD25. Thereafter, the cells were stained for intracellular expression of Foxp3 using Treg staining kit (BD Bioscience, Mississauga, ON, Canada) according the manufacturer's suggested protocol.

Confocal microscopy

PBS treated and *L. major* infected ear tissues from C57BL/6 mice were harvested after 3 days post infection. The tissues were fixed for 1h at 4°C in 4% paraformaldehyde in PBS, and incubated at 4°C for 1h in 10% and 20% sucrose in PBS, then in 30% sucrose overnight. Tissues were embedded in OCT compound (Fisher Scientific) and cut into 10 μm sections using a cryostat and mounted onto microscope slides. Slides were washed, blocked with Fc blocker (Innovex), 4% mouse serum (ImmunoReagents) and 4% goat serum. The primary antibodies used were rat anti-PTX3 (Enzo Life Sciences) at a 1:400 dilution, and rabbit anti-CD68 (Abcam) at a 1:400 dilution. Secondary antibodies used were AF568-conjugated goat anti-rat (Invitrogen) at 1:1000 dilution, and AF647-conjugated goat anti-rabbit (Invitrogen) at 1:5000 dilution. Slides were stained with Hoechst 33342 (Molecular Probes) for 30 min at 1:2000 dilution and mounted with ProLong Gold (Invitrogen). Images were acquired using the Zeiss AxioObserver confocal microscope. Colocalization analysis (using Manders' correlation coefficient) was performed using the JACoP plugin in ImageJ.

QUANTIFICATION AND STATISTICAL ANALYSIS

Results are shown as means ± SE. Results from different groups were compared using Student's t test or One-way ANOVA. A p value of ≤ 0.05 was considered significant. All of the statistical details of the experiments reported here can be found in the figure legends.